



# Engineered polylactide (PLA)–polyamide (PA) blends for durable applications: 1. PLA with high crystallization ability to tune up the properties of PLA/PA12 blends

Marius Murariu, Thomas Arzoumanian, Yoann Paint, Oltea Murariu, Jean-Marie Raquez & Philippe Dubois

To cite this article: Marius Murariu, Thomas Arzoumanian, Yoann Paint, Oltea Murariu, Jean-Marie Raquez & Philippe Dubois (2022): Engineered polylactide (PLA)–polyamide (PA) blends for durable applications: 1. PLA with high crystallization ability to tune up the properties of PLA/PA12 blends, European Journal of Materials, DOI: [10.1080/26889277.2022.2113986](https://doi.org/10.1080/26889277.2022.2113986)

To link to this article: <https://doi.org/10.1080/26889277.2022.2113986>



© 2022 The Author(s). Published by Informa UK Limited, trading as Taylor & Francis Group.



[View supplementary material](#)



Published online: 30 Sep 2022.



[Submit your article to this journal](#)



Article views: 215



[View related articles](#)



[View Crossmark data](#)

# Engineered polylactide (PLA)–polyamide (PA) blends for durable applications: 1. PLA with high crystallization ability to tune up the properties of PLA/PA12 blends

Marius Murariu<sup>a</sup>, Thomas Arzoumanian<sup>b</sup>, Yoann Paint<sup>a</sup>, Oltea Murariu<sup>a</sup>, Jean-Marie Raquez<sup>a,c</sup> and Philippe Dubois<sup>a,c</sup>

<sup>a</sup>Laboratory of Polymeric and Composite Materials (SMPC), Materia Nova Materials R&D Center – UMon Innovation Center, Mons, Belgium; <sup>b</sup>Laboratoire de Chimie-Physique Macromoléculaire (LCPM), Université de Lorraine, Nancy, France; <sup>c</sup>Center of Innovation and Research in Materials and Polymers (CIRMAP), Laboratory of Polymeric and Composite Materials (SMPC), University of Mons (UMons), Mons, Belgium

## ABSTRACT

Poly(lactide) (PLA), a biodegradable polyester produced from renewable resources, has a key position in the very promising market for bioplastics. Unfortunately, for utilization in durable/engineering applications, PLA suffers from some shortcomings such as low rate of crystallization, brittleness, and small ductility. The study proposes the use of PLA having high crystallization ability to tune up the properties of partly bio-based PLA/polyamide 12 (PA12) blends in presence of key additives. First, phenylphosphonic acid zinc salt (PPA-Zn) was selected as one of the most adapted nucleating agents (NAs) for PLA, whereas larger quantities of PLA(NA) have been produced for blending with PA12. The characterizations of PLA(NA) confirm dramatic improvements of PLA crystallization kinetics and an impressive degree of crystallinity (>40%). Blends having different PLA(NA)/PA12 ratios were prepared by melt-mixing with a laboratory micro-compounder and characterized in terms of morphology, thermal stability, and with focus on the evidence of advanced crystallization properties. All differential scanning calorimetry measurements of PLA(NA)/PA12 blends suggest powerful nucleation and crystallization ability. Furthermore, addition of epoxy-functional styrene-acrylic compatibilizers into


## ARTICLE HISTORY

Received 24 January 2022  
Accepted 12 August 2022

## KEYWORDS

Poly(lactide) or poly(lactic acid); crystallization and nucleating agents; polyamide 12 (PA12); PLA–PA blends and compatibilizers; thermal properties and morphology; durable applications

**CONTACT** Marius Murariu  [marius.murariu@materianova.be](mailto:marius.murariu@materianova.be); Philippe Dubois  [philippe.dubois@umons.ac.be](mailto:philippe.dubois@umons.ac.be)

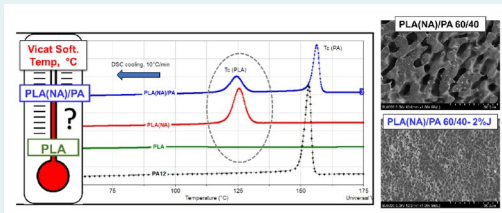
 Supplemental data for this article can be accessed online at <https://doi.org/10.1080/26889277.2022.2113986>.

© 2022 The Author(s). Published by Informa UK Limited, trading as Taylor & Francis Group.

This is an Open Access article distributed under the terms of the Creative Commons Attribution-NonCommercial License (<http://creativecommons.org/licenses/by-nc/4.0/>), which permits unrestricted non-commercial use, distribution, and reproduction in any medium, provided the original work is properly cited.

selected compositions by reactive extrusion (REX) was found to significantly change their morphology, preserving the properties of crystallization of PLA, with enhancements of mechanical properties (strength, ductility, impact resistance) confirmed by current prospects.

### GRAPHICAL ABSTRACT



## 1. Introduction

The extraordinary interest and progress in the production of biosourced polymers is connected to a large number of factors including consumer requests for eco-friendly products, the development of new bio-based feedstocks, increase of restrictions for the use of polymers with high “carbon footprint” of petrochemical origin, particularly in applications such as packaging, automotive, electrical and electronics industry, and so on (Babu, O’Connor, & Seeram, 2013; Halley & Dorgan, 2011; Koronis, Silva, & Fontul, 2013; Murariu & Dubois, 2016; Raquez, Habibi, Murariu, & Dubois, 2013; Rezvani Ghomi et al., 2021; Shaghaleh, Xu, & Wang, 2018). Moreover, important demands for biopolymers can be expected from those applications that will get clear technical and environmental benefits. Still, for many applications the carbon footprint can be reduced by decreasing or replacing the “fossil carbon” with “renewable carbon” (Tripathi, Misra, & Mohanty, 2021).

Poly(lactic acid) or polylactide (PLA), an aliphatic biopolyester produced from renewable resources, is considered as one key candidate for new developments and the growth of global production capacities in the realm. Deemed as an alternative of choice for the partial substitution of petroleum-based polymers, PLA is not only biodegradable under industrial composting conditions, but it is produced from renewable natural resources by fermentation of polysaccharides or sugar, e.g., extracted from sugarcane, corn or sugar beet, and corresponding wastes (Drumright, Gruber, & Henton, 2000; Jamshidian, Tehrani, Imran, Jacquot, & Desobry, 2010; Lim, Auras, & Rubino, 2008; Morão & de Bie, 2019; Murariu & Dubois, 2016; Rasal, Janorkar, & Hirt, 2010). Initially used in small

quantities in the biomedical sector due to its biocompatibility and biodegradation, nowadays PLA is receiving a considerable attention for single use utilization such as packaging, as well as for production of textile fibres, whereas due to its properties (high mechanical performances, low processing costs), it also finds higher attention for durable applications (Auras, Harte, & Selke, 2004; Carrasco, Pagès, Gámez-Pérez, Santana, & MasPOCH, 2010; Gupta, Revagade, & Hilborn, 2007; Lasprilla, Martinez, Lunelli, Jardini, & Filho, 2012; Murariu & Dubois, 2016; Nagarajan, Mohanty, & Misra, 2016; Raquez et al., 2013; Saini, Arora, & Kumar, 2016; Teixeira, Eblagon, Miranda, Pereira, & Figueiredo, 2021). New PLA-based materials need to be developed to allow a good balance between environment-friendliness and product properties for high-performance engineering applications (Tripathi et al., 2021). For instance, PLA shows interest for production of components for laptops, cell phones, various electronic goods, as well as of automotive parts such as floor mats and spare-tire covers (Patel, Rühle, Dorgan, Halley, & Martin, 2014).

Unfortunately, as potential substitute for petroleum-based polymers in commodity and engineering applications, PLA suffers from some shortcomings (low-thermal resistance, heat distortion temperature (HDT) and rate of crystallization, brittleness and low ductility, degradation by hydrolysis) (Rasal et al., 2010). Furthermore, specific end-use properties are required upon the application (flame retardancy, Murariu et al., 2010, 2014), antistatic to conductive electrical characteristics (Murariu & Dubois, 2016; Silva, Menezes, Montagna, Lemes, & Passador, 2019), anti-UV (Murariu, Paint, et al., 2015; Murariu et al., 2011), antibacterial or barrier properties (Pantani, Gorrasi, Vigliotta, Murariu, & Dubois, 2013), etc. Consequently, new PLA-based products (composites, nanocomposites, alloys, etc.) with improved characteristics or specific end-use properties are needed to satisfy the actual requirements of engineering applications, as well as packaging and textile materials (Hassan, Balakrishnan, & Akbari, 2013; Raquez et al., 2013).

The blending of PLA with other polymers is an efficient and cost-effective method largely used to tailor and tune-up the properties of PLA-based products. Many studies have been devoted to the synthesis, characterization, and development of various PLA-based systems, including miscible blends of poly(L-lactide) and poly(D-lactide) which generate PLA stereocomplex crystals (Luo, Fortenberry, Ren, & Qiang, 2020), binary immiscible/miscible blends of PLA with other thermoplastics (Qu, Bu, Pan, & Hu, 2018; Samuel, Raquez, & Dubois, 2013; Zhao et al., 2020), multifunctional blends comprising more components (Hashima, Nishitsuji, & Inoue, 2010; Sangroniz, Gancheva, Favis, Müller, & Santamaria, 2021; Ucpinar Durmaz & Aytac, 2022), and so on. To concern the durable

applications, PLA was already combined with different polymers of both, bio-sourced or petrochemical origin, such as PA11 (Gug & Sobkowicz, 2016; Nam & Son, 2020; Stoclet, Seguela, & Lefebvre, 2011; Ucpinar Durmaz & Aytac, 2022), polymethyl methacrylate (Gonzalez-Garzon, Shahbikian, & Huneault, 2018), polycarbonate (Tejada-Oliveros, Gomez-Caturla, Sanchez-Nacher, Montanes, & Quiles-Carrillo, 2021), polyethylene terephthalate (McLauchlin & Ghita, 2016), acrylonitrile butadiene styrene (Jo, Ryu, Ko, & Yoon, 2012), PA12 (Raj, Samuel, Malladi, & Prashantha, 2020; Zhang et al., 2012), others. It was reported that the blending of PLA with engineering polymers is an efficient way to overcome the majority of its drawbacks (Zhang et al., 2012), thus several studies have concerned the synthesis and characterization of PLA/PA blends (Gug & Sobkowicz, 2016; Nam & Son, 2020; Raj, Samuel, Malladi, et al., 2020; Stoclet et al., 2011). It is noteworthy mentioning that the polyamides (e.g., PA11 and PA12) are excellent engineering polymers due to their specific properties (possibility of utilization at low and elevated temperature, good impact strength and hydrolysis resistance, high speed of crystallization, and easy processing). The blending of bio-based, brittle and mostly amorphous PLA with semi-crystalline PAs (bio-sourced (e.g., PA11) or not (PA12)) has been reported to lead to high performance materials having improved toughness, ductility, increased HDT and better thermal resistance. As an example, PLA combined with PA11 can lead to a new family of 100% renewable materials because PA11 is also of natural origin, it is produced from castor oil (Patel et al., 2014). On the other hand, it is considered that the blends of PLA and PA are immiscible but compatible in nature (Stoclet et al., 2011), and even other authors have assumed the existence of a partial miscibility due to the hydrogen bonding between the chains of PA and PLA (Feng & Ye, 2010). Furthermore, the high compatibility in the melt state between PLA and PA having long aliphatic chains (e.g., PA12) has been stated out in some more recent studies (Raj, Samuel, Malladi, et al., 2020). Therefore, even in the absence of compatibilizers, the PLA/PA blends produced by melt-blending using twin-screw extruders are considered as interesting candidates for high-performance applications (Raj, Samuel, Malladi, et al., 2020). On the other hand, it was revealed that the engineering properties and morphology of PLA/PA blends can be significantly improved using functional compatibilizers, such as PLA-grafted maleic anhydride (Raj, Samuel, Malladi, et al., 2020). Still, by the addition of multifunctional epoxide chain extenders/compatibilizers (Joncryl®) in PLA/PA11 blends an enhanced morphology was obtained, with beneficial effects on the tensile, ductility and impact properties (Rasselet, Caro-Bretelle, Taguet, & Lopez-Cuesta, 2019; Walha, Lamnawar, Maazouz, & Jaziri, 2016).

To introduce the novelty of this work, it is important to recall that, unfortunately, the properties of PLA products are significantly affected by the low degree of crystallinity (DC) and the relatively small glass transition temperature ( $\sim 60^\circ\text{C}$ ). PLA is often in an amorphous state after any processing step by, e.g., extrusion or injection moulding (IM), showing limited or poor heat resistance (HDT) (Zhang et al., 2012). In fact, this is a kind of “Achilles’ heel”, limiting PLA use in engineering/technical applications (Murariu, Dechief, et al., 2015). This parameter (i.e., the DC) is particularly essential to control PLA degradation rate, thermal resistance, as well as mechanical and barrier properties (Wu & Wang, 2013). The low crystallinity of PLA is believed to strongly influence the final properties and to limit the applications of PLA products. This aspect has not been considered enough in the previous studies regarding the production of PLA/PA blends, mainly focussed on the melt-blending of PA with commercial PLA (Raj, Samuel, Malladi, et al., 2020; Stoclet et al., 2011), traditionally characterized by low rates of crystallization.

To the best of our knowledge, this is one of the first works which would like to propose the use of PLA designed with improved nucleating/crystallization ability to produce PLA/PA blends. Generally, it is expected that the use of PLA with nucleating agents (NAs) will lead to better thermal and mechanical properties (HDT, impact resistance, flexural strength, etc.). In addition, due to faster crystallization, fine and more uniform crystalline structure, will be facilitated the processing by extrusion or IM (e.g., shorter IM cycle times, increased productivity) (Ageyeva, Kovács, & Tábi, 2022; Harris & Lee, 2008). Furthermore, the final products will show better surface aspect, uniform shrinkage, dimensional stability at higher temperature, etc. On the other hand, the presence of PA in PLA blends can contribute to the increase of toughness, ductility, HDT, thermal resistance, etc. (Walha et al., 2016). Therefore, enhanced performances can be expected to be obtained by mixing PLA(NA) with PA, and particularly, following the crystallization of both components under specific processing conditions.

The study reports the experimental pathways followed to produce innovative PLA/PA blends by incorporating PLA having high crystallinity ability. In this goal, a commercial PLA grade was modified by melt-mixing with different NAs, for the identification of the best candidate in inducing PLA crystallization at high temperature and in achieving a high DC. This experimental step was followed by the production of PLA(NA) at larger scale and its characterization point of view crystallization ability, properties practically confirmed by IM tests.

From the category of PAs of interest (PA11, PA12, others) considered for melt-blending with PLA(NA), the study is focussed on the results

obtained with a special grade of PA12. For instance, PA12 is an interesting alternative for melt-mixing with PLA because of its low melting point (thus the possibility of processing at temperatures like the ones used for PLA), lower water absorption compared to other PAs, high tensile strength and ductility, good impact, and abrasion resistance (Chanda and Roy, 2008; Degli Esposti et al., 2021). It is also noteworthy mentioning that as alternative to the currently PA12 made from fossil sources, it is also announced the PA12 production using as raw material biobased  $\omega$ -amino-lauric acid (Degli Esposti et al., 2021). Moreover, the biodegradability of PA12 by fungi and bacteria is also reported (Rydz, Sikorska, Kyulavska, & Christova, 2014; Tomita, Hayashi, Ikeda, & Kikuchi, 2003), aspect that can be of further interest, by considering that for the instance the studies regarding the biodegradation of PLA/PA blends are missing.

The PLA(NA)/PA blends produced by melt-compounding (20, 40, 60, and 80 wt.% PA12) using a laboratory micro-compounder have been characterized using different analytical techniques to evidence their morphologies and specific properties. The adequate thermal stability of PLA(NA)/PA blends is confirmed by thermogravimetric analysis (TGA), while using the differential scanning calorimetry (DSC) measurements it was evidenced the powerful nucleation and high crystallization ability of PLA. Moreover, DSC measurements have been used to quantify and evidence the successive crystallization of PA and PLA(NA) components during cooling process. Furthermore, to tune up the morphology of PLA/PA blends (characterizations by scanning electron microscopy (SEM)), selected compatibilizers were included in the formulations considered of more interest, i.e., with higher content in PLA. Accordingly, it was revealed that the specific epoxy functional styrene-acrylate oligomers are good compatibilizers for PLA/PA blends, leading to dramatic changes of their morphology, with expected effects in the enhancement of thermo-mechanical properties. Finally, it is assumed that following the validation of optimized PLA(NA)/PA12 blends at larger scale, these developments will open new perspectives for the use of PLA-based products in durable applications (transportation, electronics, mechanical, and automotive parts).

## 2. Experimental

### 2.1. Materials

Poly(L, L-lactide)–(4032 D, NatureWorks LLC) is a PLA grade supplied with the following characteristics: specific gravity = 1.24; melting point: 155–170 °C; melt flow rate (210 °C, 2.16 kg) = 7 g/10 min. According to

the producer, the other characteristics are as follows: D isomer content = 1.4%; relative viscosity = 3.94; residual monomer = 0.14%.

PA12 Rilsamid® AMNO TLD (from Arkema) is a light and thermal stabilized IM grade of high fluidity with the following characteristics: melting temperature (DSC) = 178 °C; density = 1.02 g/cm<sup>3</sup>; melt volume rate (235 °C, 2.16 kg) = 57 cm<sup>3</sup>/10 min.

Joncryl® ADR-4300F (supplied by BASF) is an epoxy functional styrene-acrylate oligomeric chain extender and compatibilizer for PAs and polyesters, having mild-epoxy functionality (Murariu, Paint, et al., 2015). According to the technical sheet of this product, it has the molecular weight ( $M_w$ ) = 5500, epoxy equivalent by weight = 445 g/mol and a glass transition temperature of about 56 °C. It will be mentioned hereinafter as “Joncryn” and it will be abbreviated as “J”.

XIBOND™ 140 (supplied by Polyscope Polymers) is a random copolymer of styrene and maleic anhydride designed to improve the morphology of specific polymer blends. Abbreviated below as “XB”, it is traditionally used as compatibilizer, coupling agent, adhesion promoter, and viscosity modifier.

Ultranox 626 A (Bis (2,4-di-*t*-butyl phenyl) pentaerythritol diphosphite) supplied by Brenntag NV (abbreviated as U626) was selected as the thermal stabilizer and used at a preferred percentage of 0.3 phr (parts per hundred parts of resin) in PLA/PA blends. Table 1 introduces the products that have been tested in the first part of the study as NAs for PLA.

**Table 1.** Products evaluated as nucleating agents (NAs) for PLA.

Code	Product	Supplier	Short description
NA1	Ecopromote	Nissan Chemical Industries, Ltd.	Phenylphosphonic acid zinc salt (PPA-Zn) of 2-3 μm as granulometry; Onset of thermal degradation >500 °C.
NA2	Sodium benzoate	Brenntag	Sodium salt of benzoic acid, nucleating agent (additive) especially used in polypropylene, polyesters (PET).
NA3	Bruggollen P252	Brüggemann Chemical	Synergistic mixture of various nucleating and lubricating products (proprietary composition). Crystallization accelerator for thermoplastic polyesters (allows PET recrystallization at about 197 °C (DSC)).
NA4	Talc JetFine® 3C A	Imerys Talc	Mg <sub>3</sub> Si <sub>4</sub> O <sub>10</sub> (OH) <sub>2</sub> , high aspect ratio, it improves the nucleation in crystalline polymers. Median diameter – d <sub>50</sub> = 3.9 μm; Surface area (BET) = 14.5 m <sup>2</sup> /g.
NA5	Talc Crys-Talc 7C	Imerys Talc	Mg <sub>3</sub> Si <sub>4</sub> O <sub>10</sub> (OH) <sub>2</sub> , micro-lamellar talc for polymer reinforcement and nucleation (PA, PLA, etc.). Granulometry by sedimentation (d <sub>50</sub> ) = 1.9 μm; Surface area (BET) = 16.9 m <sup>2</sup> /g.



## **2.2. Production of PLA(NA) and related PLA(NA)/PA blends**

### **2.2.1. Selection of NAs**

Before mixing by melt-compounding, PLA and all products tested as NAs have been dried overnight at 80 °C using an oven with recirculating hot air. For the selection of the most adapted NA, PLA was mixed with 1 wt.% NA, by shaking both components (granules and NA powder) into glass ampoules. The melt-compounding of blends (7 g of each composition) was performed at 200 °C using a conical intermeshing corotating twin-screw micro-compounder Minilab II Haake Rheomex CTW5 – Thermo Fischer Scientific, and the following specific conditions: time of feeding of 3 min at 30 rpm, mixing in recirculating mode using the back-flow channel for 7 min at 150 rpm, the speed of screws.

### **2.2.2. Melt-compounding of PLA with NA**

Following the selection of the most effective NA, i.e., phenylphosphonic acid zinc salt (PPA-Zn), in the subsequent experimental step a larger quantity of PLA containing 1 wt.% NA, and noted as PLA(NA), was prepared by melt-compounding using a Leistritz twin-screw extruder equipment (ZSE 18 HP-40, L/D=40, diameter (D) of screws = 18 mm). According to the conventional method, the PLA granules were mixed in a turbo-mixer with 1 wt.% NA (PPA-Zn), step followed by the direct feeding of the blend in the extruder. Conditions of melt-compounding: the speed of the screws = 100 rpm; the temperatures of extrusion on the heating zones were adapted to the rheological characteristics of PLA (Z1 = 185 °C; Z2 = 195 °C; Z3 = 210 °C; Z4–Z6 = 200 °C; Z7 = 195 °C).

### **2.2.3. Production of PLA(NA)/PA12 blends**

In the second part of the experimental program, samples of different PLA(NA)/PA weight ratios (100/0, 80/20, 60/40, 40/60, 20/80, and 0/100) have been produced by melt-compounding using the twin-screw micro-compounder. The compositions and codification of samples are shown in [Table 2](#). The melt-compounding of PLA(NA)/PA12 dry-mixed blends (7 g of each composition, 0.3 phr U626A added as thermal stabilizer) was performed at 200 °C using a similar procedure such as in the case of PLA–NA blends. The equipment has been controlled using the separate manual control box. To have first information about the rheology/viscosity of blends, the initial and final torque values have been noted from the screen of the control box, respectively, at the beginning and the end of mixing by 150 rpm. For the sake of comparison, PLA(NA) and PA12 have been processed in similar conditions, whereas a PLA50–PA50 sample was additionally realized for more insight regarding the evolution of morphology.

**Table 2.** Codes of PLA(NA)/PA12 samples and their composition.

Code of sample	PLA(NA), wt.%	PA12, wt.%	Compatibilizer, wt.%
PLA(NA)	100	0	–
PLA80-PA20	80	20	–
PLA60-PA40	60	40	–
PLA40-PA60	40	60	–
PLA50-PA50 <sup>a</sup>	50	50	–
PLA20-PA80	20	80	–
PA12	0	100	–
PLA60-PA40/2J	58.8	39.2	2
PLA60-PA40/2XB	58.8	39.2	2

<sup>a</sup>The PLA50-PA50 sample was realized and characterized only by SEM to have more information about the evolution of morphology of PLA-PA blends.

## 2.3. Methods of characterization

### 2.3.1. Thermogravimetric analysis

TGA was performed using a TGA Q50 (TA Instruments, New Castle, DE, USA) at a heating rate of 20 °C/min under air, from room temperature up to max 800 °C (platinum pans, 60 cm<sup>3</sup>/min air flow rate).

### 2.3.2. Differential scanning calorimetry

DSC measurements were performed by using a DSC Q200 from TA Instruments under nitrogen flow. The procedure was as follows: first heating scan at 10 °C/min from 0 °C up to 200 °C or 220 °C (in the case of samples containing PA), isotherm at these temperatures for 2 min, then cooling by 10 °C/min to –20 °C and finally, second heating scan from –20 °C to 200 °C or 220 °C at 10 °C/min. The first scan was used to erase the prior thermal history of the samples. The events of interest linked to the crystallization of PLA and PA during DSC cooling scans, i.e., the crystallization temperatures ( $T_c$ ) and the enthalpies of crystallization ( $\Delta H_c$ ), have been quantified using TA Instruments Universal Analysis 2000 software. Noteworthy, all data were normalized to the amounts of PLA or PA from the samples (Raj, Samuel, Malladi, et al., 2020). The DC was determined by considering a melting enthalpy of 93 J/g for 100% crystalline PLA (Yoo, Jeong, & Choi, 2021) and of 209 J/g for PA12 (Wei et al., 2019). Additional thermal parameters (mostly linked to PLA) were obtained from the second DSC heating scan and abbreviated as follows: glass transition temperature ( $T_g$ ), cold crystallization temperature ( $T_{cc}$ ), enthalpy of cold crystallization ( $\Delta H_{cc}$ ), peak of melting temperature ( $T_m$ ), melting enthalpy ( $\Delta H_m$ ), and the final DC ( $\chi_f$ ). Noteworthy, the DC was calculated by subtracting the enthalpies of cold crystallization ( $\Delta H_{cc}$ ) and of pre-melt crystallization (if they are evidenced on DSC curves), from the enthalpies of melting ( $\Delta H_m$ ).

Screening tests to evaluate the crystallization kinetics of PLA were performed through the determination of crystallization half-time ( $t_{1/2}$ ) during isothermal crystallization. Using DSC, selected PLA samples were heated to 200 °C at a rate of 10 °C/min, held for 2 min at this temperature to erase their thermal history, step followed by high-speed cooling (about 40 °C/min) to the iso-crystallization temperature of interest (typically in the range 110–130 °C), and maintained under isothermal conditions for up to 120 min (the starting neat PLA requires a long testing time). The relative crystallinity was calculated by integrating the total area under the curve for each crystallization exotherm, whereas  $t_{1/2}$  was taken to be the time at which the relative crystallinity (area) was equal to 50%.

### **2.3.3. Tests by IM to evidence the crystallization ability of PLA(NA)**

The IM technique was used to practically highlight the increase of DC in the case of PLA(NA) samples by comparing to the neat PLA. PLA(NA) and neat PLA were processed by IM using a DSM micro-IM machine (5.5 cm<sup>3</sup>) with the barrel temperature set at 200 °C to produce thin specimens, typically of 1.5 mm thickness. The IM tests were performed using a residence time in the mould of 1 or 2 min, and different temperatures of the mould: 30–40 °C (no heating); 80 °C; 100 °C and 120 °C. The values of the DC after IM were determined by DSC analysis by quantifying the thermal events from the first DSC scan.

### **2.3.4. Scanning electron microscopy**

SEM analyses on the previously cryofractured samples at the liquid nitrogen temperature were performed by using a SU8020 scanning electronic microscope (Hitachi) at a typical accelerated voltage of 5 kV and at various magnitudes. For better information and easy interpretation of morphology, SEM analyses were also performed on samples of PLA/PA previously etched in chloroform (for max. 60 min), solvent typically used to selectively dissolve PLA. The measurements of the size of PA or PLA domains representing the “minor” phase (into PLA or PA as matrices, respectively) were realized using the ImageJ 1.52d software for analysing scientific images (National Institutes of Health, Bethesda, MD, USA).

## **3. Results and discussion**

### **3.1. Production and characterization of PLA(NA)**

Unfortunately, PLA use in durable applications is limited when compared to other thermoplastics (polycarbonate, polyamide, polystyrene, etc.), due to its relatively low  $T_g$  and small rate of crystallization, or even to the

lack of crystallinity after a fast processing, e.g., by IM (Jiang et al., 2016; Murariu, Dechief, et al., 2015). In order to increase the crystallization rate and the DC of PLA, different techniques are practically applied, such as adding NAs, blending with plasticizers, minimizing the D-lactide content in PLA (using PLA grades mostly containing L-lactide repeating units), adjusting IM parameters (processing temperature and moulding time) (Chen et al., 2015), post-annealing, etc. More details about the current methods used to increase the crystallization rate (DC) of PLA can be found in a previous study published by our group (Murariu, Dechief, et al., 2015). Mineral NAs (talc, clays, etc.), organic additives such as hydrazide compounds and organic-mineral hybrids such as layered metal phosphonates can increase the number of primary nucleation sites, reducing the nucleation induction period, and initiate PLA crystallization at higher temperature during cooling from the melt (Saeidlou, Huneault, Li, & Park, 2012).

### 3.1.1. Selection of NA

In this study, five products potentially claimed as NAs have been considered to increase the crystallization kinetics of PLA: NA1 is a PPA-Zn (Ageyeva et al., 2022; Chen et al., 2015; Suryanegara, Okumura, Nakagaito, & Yano, 2011), NA4 and NA5 are two grades of talc having different granulometry, mineral fillers with lamellar structure largely recognized to accelerate the crystallization rate of PLA (Battezzore, Bocchini, & Frache, 2011; Harris & Lee, 2008; Shakoor & Thomas, 2014). Sodium benzoate (NA2) was considered as being of interest based on some sources of literature (Penco et al., 2011), while NA3 (proprietary composition) (Wypych & Wypych, 2021) is mentioned as a highly efficient NA for polyesters (i.e., PET). Going from the information provided by the state of the art (Ageyeva et al., 2022; Li & Huneault, 2007; Nagarajan et al., 2016; Wypych & Wypych, 2021), for convenience and only for comparative reasons, all PLA compositions performed in the frame of the experimental program contain 1% NA.

One key objective was to select the NA which allows PLA crystallization at high temperature during cooling from the molten state, and more preferably, near  $T_c$  of PA12. It was also assumed that DSC is probably the simplest technique which could give relevant and fast information about the crystallization properties of PLA products, by studying their non-isothermal and isothermal crystallization (Battezzore et al., 2011; Harris & Lee, 2008; Murariu, Paint, et al., 2015).

Figure 1(a, b) shows the representative DSC curves of PLA-NA1-5 samples and of starting neat PLA recorded respectively, during cooling from the molten state (rate of 10 °C/min) after erasing the prior thermal

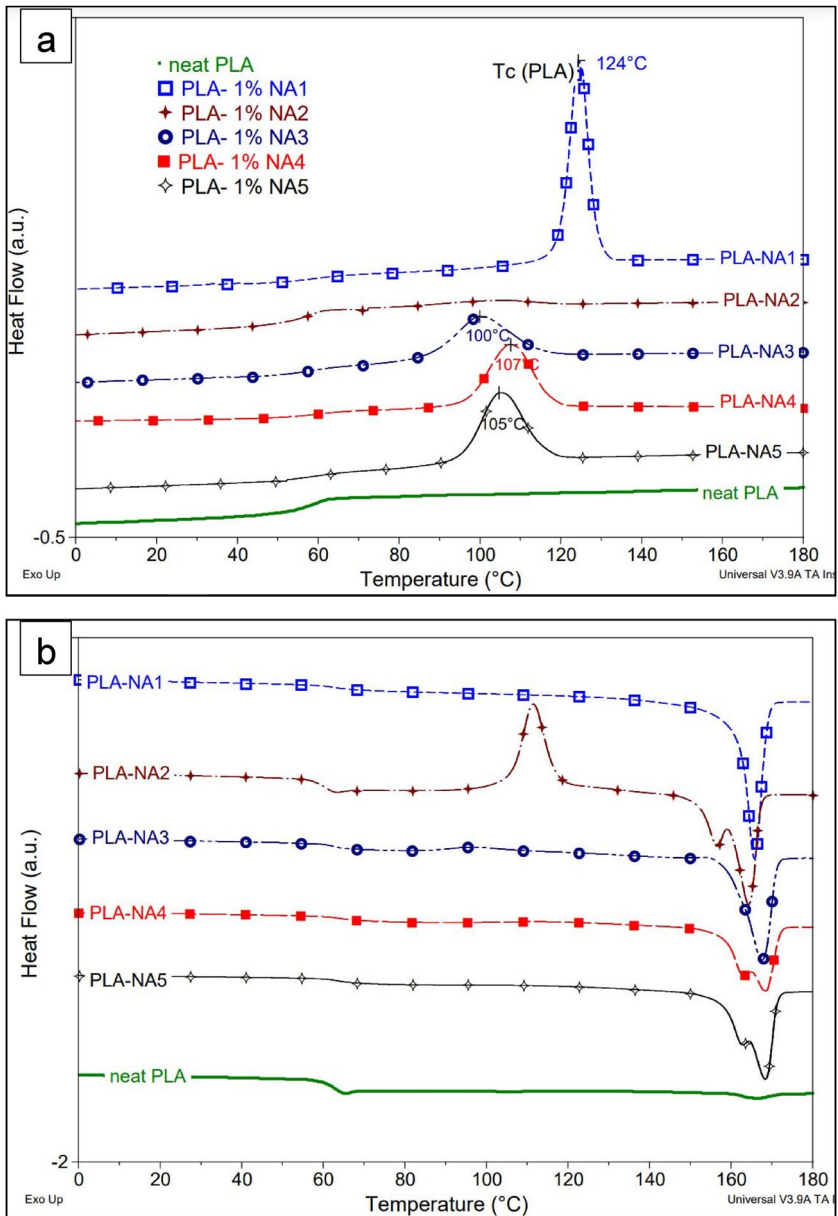


**Figure 1.** Comparative DSC traces of starting neat PLA and of PLA-NA1-5 samples recorded (a) during cooling and (b) second heating (rate of 10°C/min).

history by a first heating scan, and those obtained during the second DSC heating (the quantification of data is shown in Table 3). By considering the non-isothermal crystallization of PLA-based samples (Figure

**Table 3.** Comparative DSC data on starting PLA and PLA-NA1-5 samples obtained during non-isothermal crystallization from the molten state (cooling by 10 °C/min) and following the succeeding heating scan.

Sample	DSC cooling by 10 °C/min			Second DSC heating scan, 10 °C/min					
	$T_c$ °C	$\Delta H_c$ J/g	$\chi_c$ %	$T_g$ °C	$T_{cc}$ °C	$\Delta H_{cc}$ J/g	$T_m$ °C	$\Delta H_m$ J/g	$\chi_f$ %
Neat PLA (AR)	–	–	–	63	–	–	167	1.9	2.0
PLA-1% NA1	124	37.9	40.7	62	–	–	166	39.1	42.0
PLA-1% NA2	–	–	–	60	111	27.0	157; 164	38.3	12.2
PLA-1% NA3	100	21.5	23.1	62	97	3.0	167	33.4	32.7
PLA-1% NA4	107	25.5	27.4	63	–	–	163; 168	27.2	29.2
PLA-1% NA5	105	27.8	29.9	64	–	–	163; 168	32.7	35.2

**Abbreviations:** DSC cooling: crystallization temperature ( $T_c$ ), enthalpy of crystallization ( $\Delta H_c$ ) and corresponding degree of crystallinity ( $\chi_c$ ); Second DSC heating: glass transition temperature ( $T_g$ ), cold crystallization temperature ( $T_{cc}$ ), enthalpy of cold crystallization ( $\Delta H_{cc}$ ), melting temperature ( $T_m$ ), enthalpy of fusion ( $\Delta H_m$ ), final degree of crystallinity ( $\chi_f$ ).

1(a)), it is noted that, at the exception NA2 (sodium benzoate), all other products (NA1, NA3, NA4, and NA5) are clearly leading to an important gain of crystallinity during cooling, revealed by the important exothermal events ascribed to the crystallization of PLA. For instance, using NA1 it is noticeable that the peak of crystallization ( $T_c$ ) is recorded at about 124 °C, while using NA3 the  $T_c$  is noted at lower temperature ( $T_c \approx 100$  °C). Regarding the effects of talc of different granulometry (NA4 and NA5, have a  $d_{50}$  of 3.9  $\mu\text{m}$  and 1.9  $\mu\text{m}$ , respectively), the  $T_c$  is in the range 105–107 °C, which means some lower effectiveness compared to NA1 (PPA-Zn). Furthermore, the DC achieved during crystallization from the melt is much impressive using NA1 (40.7%) compared to the other NAs (values <30%). Still, in the subsequent DSC heating scan, the samples that are well crystallized during cooling (NA1, NA4, NA5) do not show any significant cold crystallization, while the increases of crystallinity are minor. From the quantification of enthalpies recorded during cooling ( $\Delta H_c$ ) and in the second heating ( $\Delta H_m$ ), and following the determination of DC, it comes out that the presence of NA1 into PLA allows a gain of crystallinity higher than 40%, which demonstrates an impressive effectiveness in promoting PLA crystallization. On the other hand, it is noteworthy mentioning that the neat PLA (granules as received (AR), not processed) does not show any detectable crystallization, thus only a low DC (2%) is calculated after the second DSC heating scan. Comparable results (i.e., a DC of 0.9%) were reported elsewhere by Yoo et al. (2021), following the characterization by DSC of a similar PLA grade.

Regarding the other thermal properties displayed in Table 3, there are not any significant changes of  $T_g$ , whereas from the profile of endotherms of fusion (showing one or two melting peaks), obviously, this could raise

a larger discussion about the presence of crystalline structures of different perfection.

Besides, by considering the overall results and objectives (crystallization from the melt at elevated temperature (high  $T_c$ ) and high level of crystallinity), the following order of effectiveness can be suggested: NA1 > NA5  $\approx$  NA4 > NA3  $\gg$  NA2.

Finally, NA1 (PPA-Zn) was considered as the best alternative in inducing PLA crystallization, therefore it was then used for the production, via a pilot twin-screw extruder (see the experimental part), of larger quantities of PLA added with 1 wt.% of PPA-Zn, that will be noted as PLA(NA) in the following sections. PLA(NA) will also be used as main raw material for melt-mixing with PA12.

Figure 2 shows the comparative DSC traces (cooling from the melt state and second heating scan) of starting PLA and of so produced PLA(NA). PLA(NA) exhibits a sharp peak of crystallization ( $T_c$  about 125°C) and an important enthalpy of crystallization during cooling, whereas following the second heating scan, obviously it is (re)confirmed its impressive DC compared to that of neat PLA (i.e., 40.5% compared to 2%, respectively).

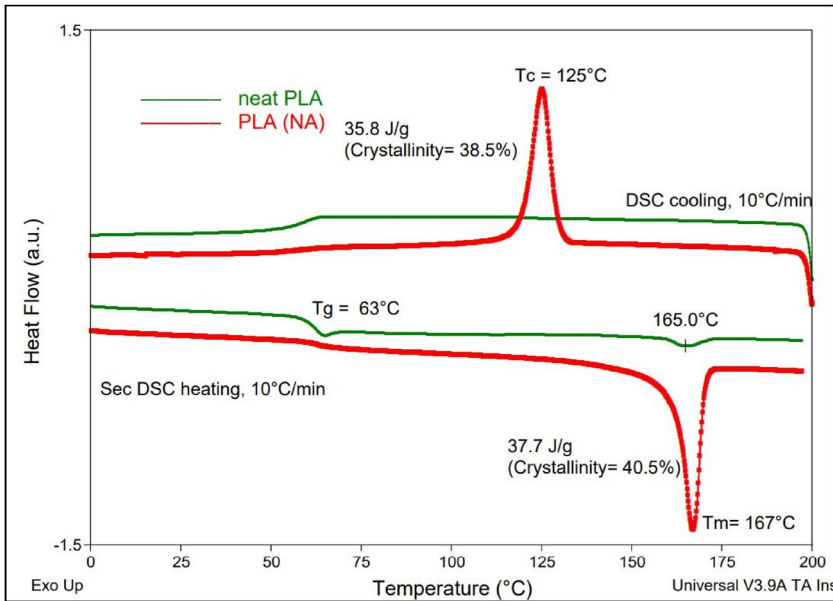


**Figure 2.** Comparative DSC curves of starting PLA and PLA(NA) displayed during cooling and second heating scan at rate of 10°C/min and quantification of the main information.

### 3.1.2. Isothermal crystallization of PLA(NA) and IM experiments

To evidence the effectiveness of PLA(NA) from the point of view of crystallization ability, DSC isothermal crystallization experiments were carried out for the determination of crystallization half-time ( $t_{1/2}$ ), i.e., the time consumed to reach 50% of final crystallinity. It is worth mentioning that the products that show capability to nucleate PLA have a dramatic contribution in the decreasing of  $t_{1/2}$ . Crystallization exotherms were measured as a function of time and the  $t_{1/2}$  was determined as reported elsewhere (Harris & Lee, 2008). PLA(NA) shows intense and narrow exotherms (Figure 3) at the temperature of 120 °C and 130 °C (a  $t_{1/2}$  of only 0.3 min and 0.6 min, respectively), while the neat PLA displayed much broader traces. In fact, the neat PLA (granules, AR) shows a high  $t_{1/2}$  (higher than 60 min at the temperature of 120 °C), above 50 min at 110 °C (see the inset of Figure 3), which attests for the low crystallization ability of this polyester. The results are in good agreement with the values currently reported in literature using similar methods (Harris & Lee, 2008; Li & Huneault, 2007; Murariu, Dechief, et al., 2015; Yoo et al., 2021). For the same grade of PLA, Yoo et al. (2021) have reported a  $t_{1/2}$  of 36 min and 52 min, at the temperatures of crystallization of respectively, 110 °C and 120 °C. Moreover, Li and Huneault (2007) have concluded that the pure PLA (4032D) has a very slow crystallization

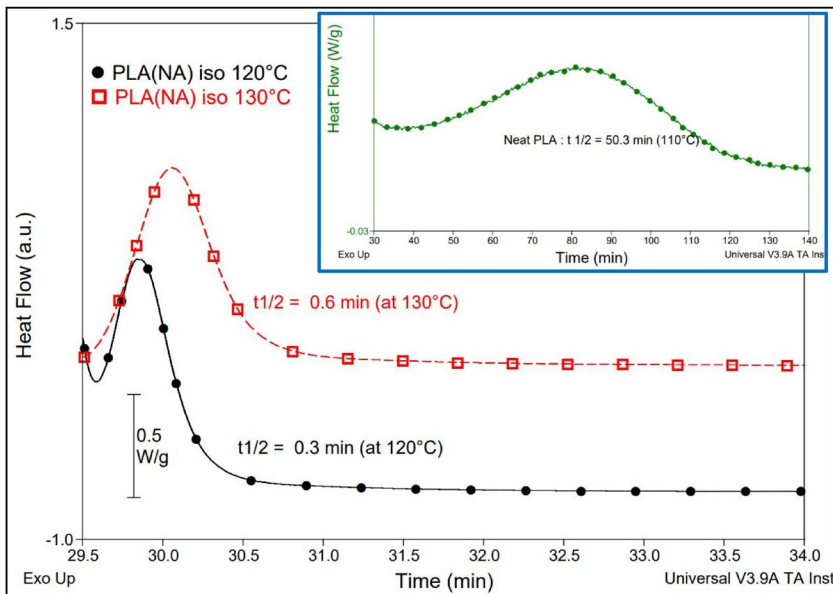


**Figure 3.** DSC traces obtained during crystallization of PLA(NA) under isothermal conditions for determination of half crystallization time ( $t_{1/2}$ ). In the inset of figure: isothermal crystallization of starting neat PLA at 110 °C assessing for a very long  $t_{1/2}$ .



rate, and the minimum  $t_{1/2}$  is around 40 min at an optimum temperature of 100 °C. It is worth also reminding that the  $t_{1/2}$  of the PLA depends on crystallization temperature, content of enantiomeric impurities (i.e., D-isomer) in PLA, molecular weights, and processing parameters. For instance, Battagazzore et al. (2011) have reported a  $t_{1/2}$  of 82 min for a PLA containing 4% D-isomer following its isothermal crystallization at 110 °C. Still, it is important to mention that the kinetics of crystallization of neat PLAs are enhanced following their processing or melt-compounding with/without additives (e.g., under medium/high shear conditions), therefore the  $t_{1/2}$  can be significantly decreased (Murariu, Dechief, et al., 2015), but it remains much higher than in the presence of NAs.

On the other hand, very interesting information regarding the crystallization properties of PLA can be obtained via IM experiments (Harris & Lee, 2008; Murariu, Paint, et al., 2015). Figure 4(a, b) shows the DSC traces obtained during first heating scan of the injection moulded PLA(NA) samples annealed in the mould for 1 and 2 min (at 30–40 °C; 80 °C; 100 °C; 120 °C), while for comparison Figure 4(c) shows those of neat PLA, at 2 min annealing time. Obviously, in the case of neat PLA, even at longer residence time (2 min) and high temperature of the mould (i.e., 100 °C and 120 °C), the DC remained relatively low, in the range 10–15% (Table 4). On the contrary, PLA(NA) annealed in the mould (1–2 min at 100–120 °C) shows unconventional crystallization ability, and consequently, an increased DC (38–47%). It is also noticed that at lower temperature (<80 °C) the effectiveness of NA is much decreased. Furthermore, in all cases on the DSC curves of PLA (Figure 4(c)), an important process of cold crystallization is observed, while for PLA(NA) this exothermic event is missing, if the temperature of the mould is higher than 100 °C. To conclude in relation to the IM experiments, PLA(NA) leads to a noteworthy DC at shorter residence time in the mould (mould temperature of 100–120 °C), assumed to be even lower than 1 min, as it comes out from the determination of  $t_{1/2}$ .

Accordingly, PPA-Zn acts as a powerful NA, increasing the crystallization kinetics of PLA during IM process. This is in perfect agreement with the results of other studies where PPA-Zn was reported as an effective site of heterogeneous nucleation, increasing the nucleation density of PLA, and acting as flat surface side for the growth of PLA crystals (Chen et al., 2015; Kusumi et al., 2018). Moreover, regarding the crystallization kinetics of PLA in the presence of PPA-Zn, the nucleation mechanism and crystal growth, more information can be obtained from the paper of Wu and Wang (2013) that have investigated both, the non-isothermal cold and isothermal melt crystallization of PLA with different amounts of PPA-Zn at various crystallization temperatures, by DSC and polarized optical microscopy (POM) measurements. Characterized by

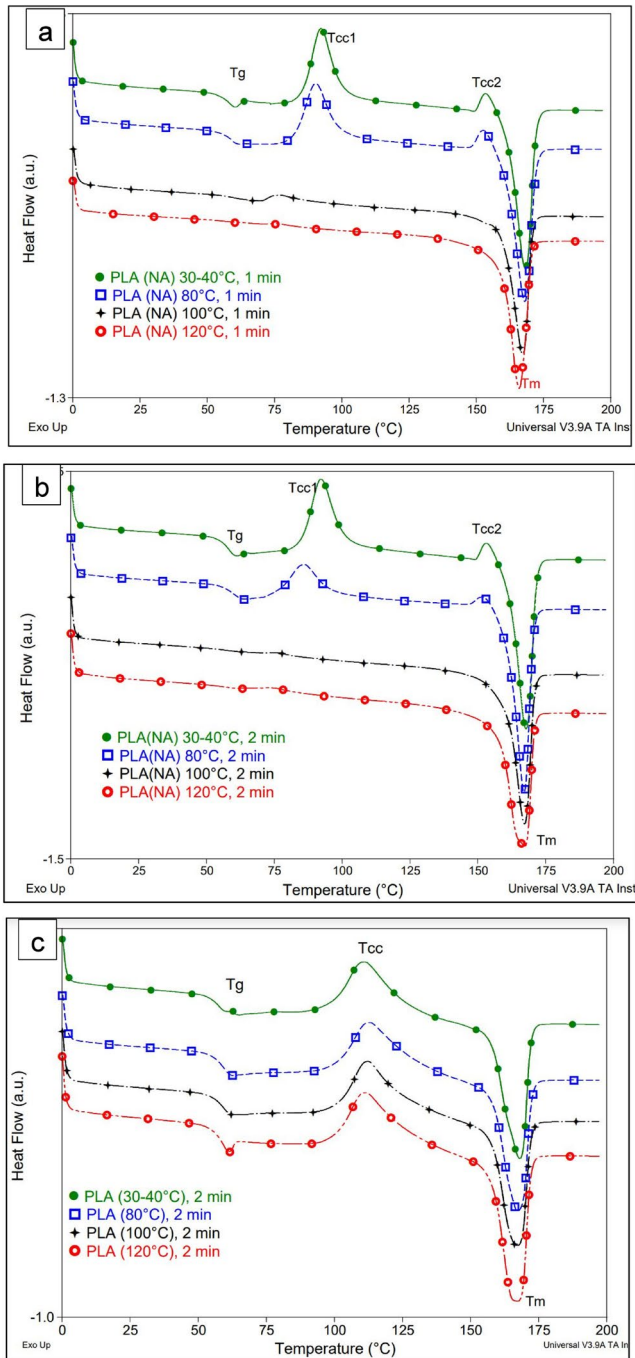


**Figure 4.** Comparative DSC curves of (a, b) PLA(NA) and (c) neat PLA after IM at different temperatures of the mould and distinct residence time.

**Table 4.** Degree of crystallinity (%) of neat PLA and PLA(NA) following the processing by injection moulding at different mould temperatures.

Sample	Residence time, min ↓	Degree of crystallinity, % (at the temperature of the mould given hereunder)			
		30–40 °C	80 °C	100 °C	120 °C
PLA(NA)	1	13.1	15.2	38.2	46.3
	2	15.9	27.4	40.2	46.7
Neat PLA	2	8.0	9.1	10.2	15.1

high tensile strength and rigidity, but low ductility (see the Section 3.3, current prospects), it is assumed that PLA(NA) items produced by IM under optimized conditions will assess a high DC, fine and more uniform crystals, with beneficial effects in improved processing and in obtaining better performances, such as heat resistance and gas-barrier properties.

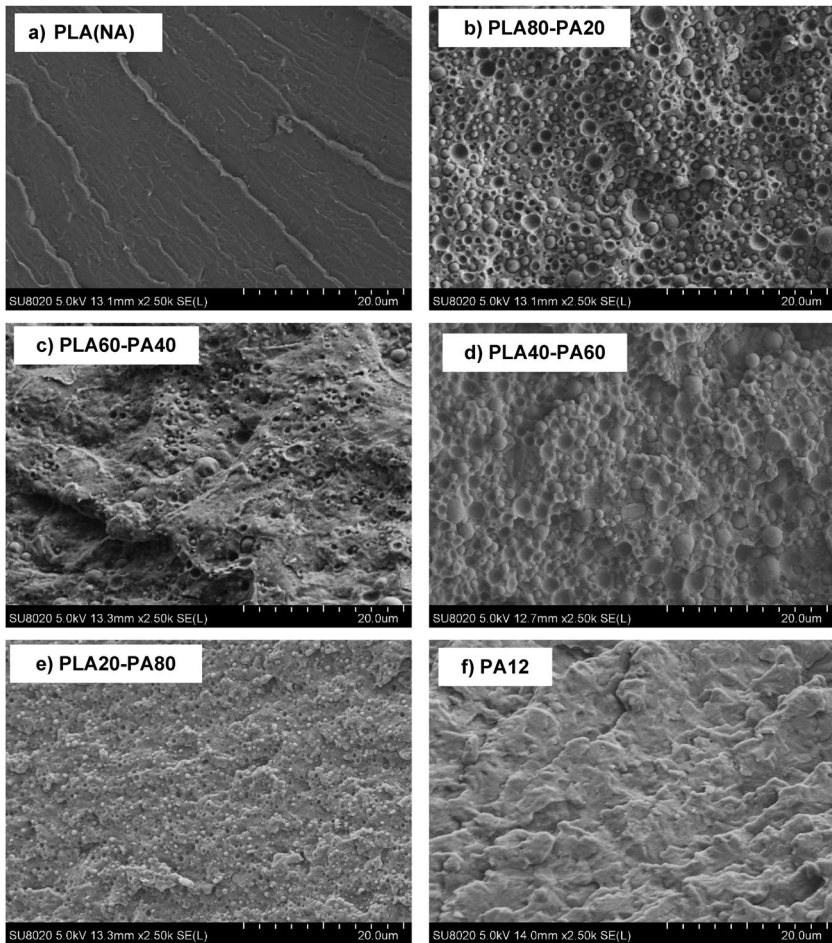
### 3.2. Production and characterization of PLA(NA)/PA12 blends

PLA(NA)/PA12 blends have been produced using a conical intermeshing corotating twin-screw micro-compounder (see experimental part, Table 2) and characterized to have information about their thermal stability, morphology, and properties of crystallization.

It is worth pointing out that the melt viscosity of PLA is higher than that of PA12 under the conditions of melt-compounding, and this is first confirmed by the values of torque (beginning and end of mixing) as primary rheological information. For shortness, these results and brief comments are shown elsewhere (Supplementary material, Figure S1).

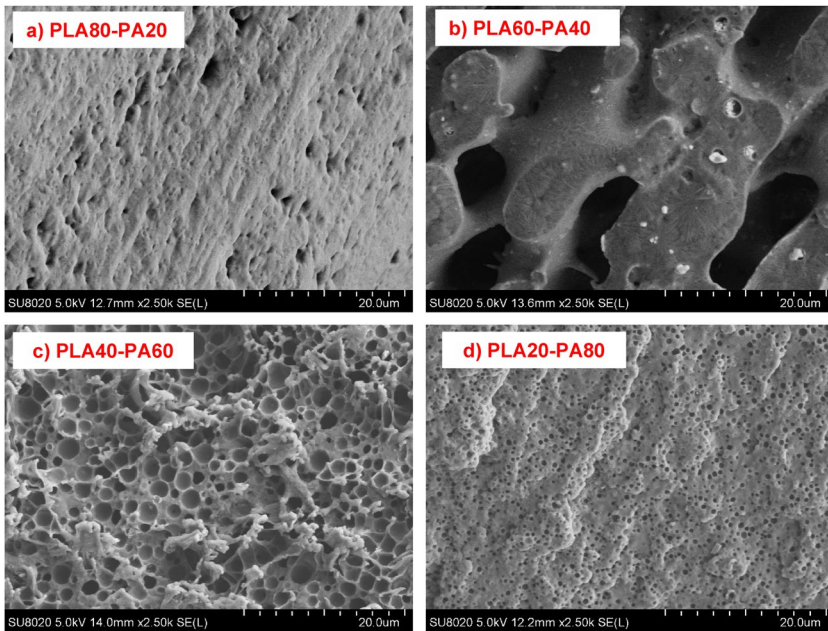
#### 3.2.1. Morphology of PLA(NA)/PA12 blends

Figure 5(a–f) shows the images of cryofractured surfaces of PLA(NA), PA12 and their PLA/PA blends. First, due to the immiscible nature of PLA/PA12 blends, where the minor component is up to 20 wt.% (i.e., PLA80-PA20 and PLA20-PA80 samples), a sea-island morphology with “droplets” that are uniformly distributed within PLA or PA matrix is observed in SEM images (Figure 5(b, e), respectively). Interestingly, under the experimental conditions of melt-mixing, the dimension of spherical particles is significantly higher when PA is the minor phase in PLA as matrix ( $1.2 (\pm 0.4) \mu\text{m}$ ), by comparing to  $0.6 (\pm 0.1) \mu\text{m}$  for the blends when PLA is the minor component dispersed through PA as matrix. However, by increasing the amounts of PA to 40–60 wt.% it is expected to have the evidence of co-continuous morphology, which is usually obtained for symmetric compositions, particularly for components having



**Figure 5.** (a–f) SEM micrographs of cryofractured surfaces of PLA(NA), PA12, and PLA(NA)/PA samples.

similar viscosities and density (Fenni, Cavallo, & Müller, 2019). On the other hand, the SEM micrographs of PLA40-PA60 samples containing 60 wt.% PA confirm the presence of “nodules” of PLA (40 wt.%) dispersed within PA matrix (Figure 5(d)). This allows concluding that the phase inversion (PI) point must be found for the blends having higher PLA percentage. Moreover, additional confirmation is obtained from the SEM analyses (Figure 6(a–d)) of “etched” samples in chloroform (a selective solvent for PLA phase). Accordingly, the SEM micrographs of PLA40-PA60 blends (Figure 6(c)) clearly highlight the presence of round-shaped domains of PLA (diameter of  $1.8 \pm 0.5 \mu\text{m}$ ) which are uniformly distributed through the PA matrix, the polymer of lower viscosity. On the other



**Figure 6.** (a–d) SEM micrographs of PLA(NA)/PA12 samples previously “etched” in chloroform.

hand, a co-continuous structure is well evidenced as morphology for PLA60–PA40 samples (Figure 6(b)), i.e., blends containing 60 wt.% PLA. However, it is assumed that the region of co-continuity can be larger (Jalali Dil, Carreau, & Favis, 2015). Thus, for better insight and additional information regarding the zones of co-continuity and PI, a PLA50–PA50 blend has been prepared, and supplementary characterized by SEM (Figure 7(a, b)). Accordingly, the PI (PLA passes into PA phase) is clearly evidenced at 50 wt.% PLA in the blends (Figure 7(a)), with PLA domains of low or larger size. Similar results are reported by Stoclet et al. (2011) for PLA/PA11 blends, PLA appearing to be dispersed as “globules” within PA matrix, at PLA amounts below 50 wt.%. On the other hand, linked to the co-continuity range, it was reported that the PLA/PBAT blends can show a wide and symmetrical region of co-continuity, with the lower and upper limits located between 30–40 and 60–70 vols.% of PBAT, respectively (Jalali Dil et al., 2015).

Figure 8 summarizes the different morphologies obtained by increasing the amounts of PA12 in PLA(NA)/PA blends. Finally, by considering that the results obtained in the frame of different studies can have some specificity, it is worth noting that there is some consensus regarding the morphologies of PLA/PA blends, especially obtained at increased amounts of PLA or PA. On the other hand, by introducing

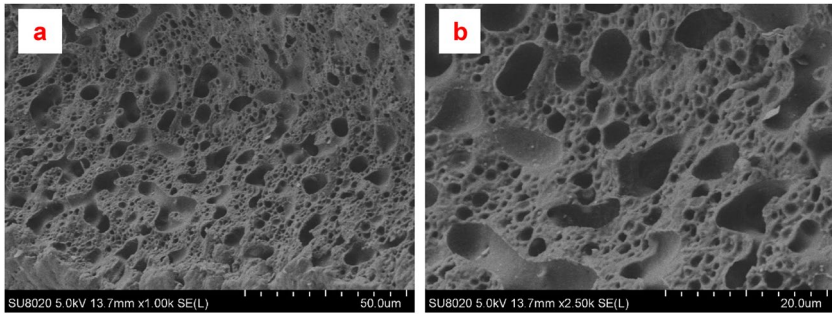


**Figure 7.** (a, b) SEM micrographs of previously “etched” PLA50-PA50 samples to illustrate the inversion of the phase (PLA pass into PA as matrix).

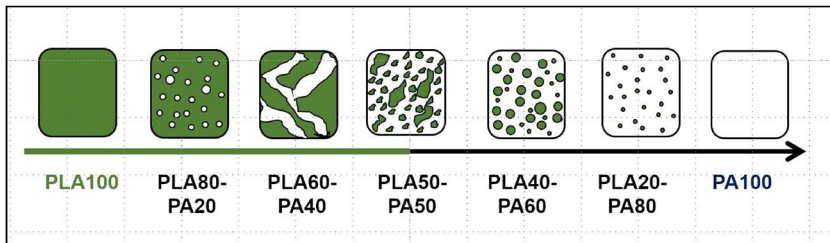


**Figure 8.** Scheme to illustrate the morphology evolution by increasing the amounts of PA12 in PLA(NA)/PA blends.

the constraints linked to a high amount of bio-renewable carbon (blends rich in PLA), the opinions and tendencies are less clear, thus more efforts should be addressed to the identification of compositions and processing conditions that will provide optimal performances in engineering applications.

### 3.2.2. TGA of PLA(NA)/PA blends

First, from the evolution of TG and D-TG curves (Figure 9(a, b)) is seen that PA12 is characterized by higher thermal stability than that of PLA ( $T_{5\%}$ , considered the onset of thermal degradation, is 393 °C and 337 °C, respectively – data shown in Table 5). Thus, adding and increasing the loading of PA in PLA/PA blends will lead to compositions with improved thermal parameters. However, from the profiles of D-TG curves (Figure 9(b)), it is noticed the presence of two distinct zones of thermal degradation, at a temperature of about 370 °C corresponding to the degradation of PLA ( $T_{d1}$ ), and in the range 440–470 °C, ascribed to the degradation of PA ( $T_{d2}$ ). Still, there is a slight increase of  $T_{5\%}$  especially for the blends which are rich in PA. Nevertheless, by considering as a

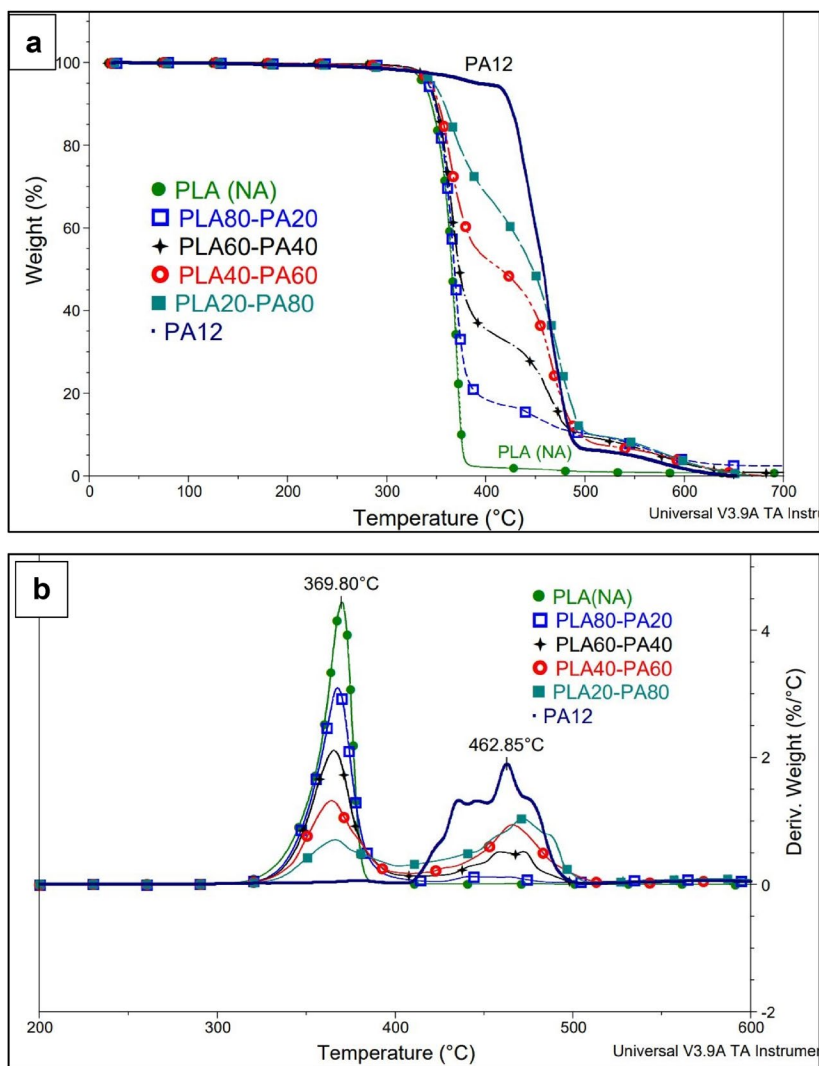


**Figure 9.** TG (a) and D-TG curves (b) of PLA(NA), PA12, and PLA/PA blends (under air, 20°C/min).

**Table 5.** Thermal parameters of PLA(NA), PA12 and PLA(NA)/PA blends as determined by TGA.

Sample code	$T_{5\%}$ , °C	Weight loss up to 400°C, %	$T_{d1}$ , °C (PLA)	$T_{d2}$ , °C (PA)
PLA(NA)	337	98	370	–
PLA80-PA20	341	81	367	442
PLA60-PA40	342	65	365	467
PLA40-PA60	344	47	364	466
PLA20-PA80	348	29	362	472
PA12	393	6	–	463

parameter the weight loss at 400°C, it appears more evident the beneficial contribution of PA component in limiting the degradation of PLA/PA blends.

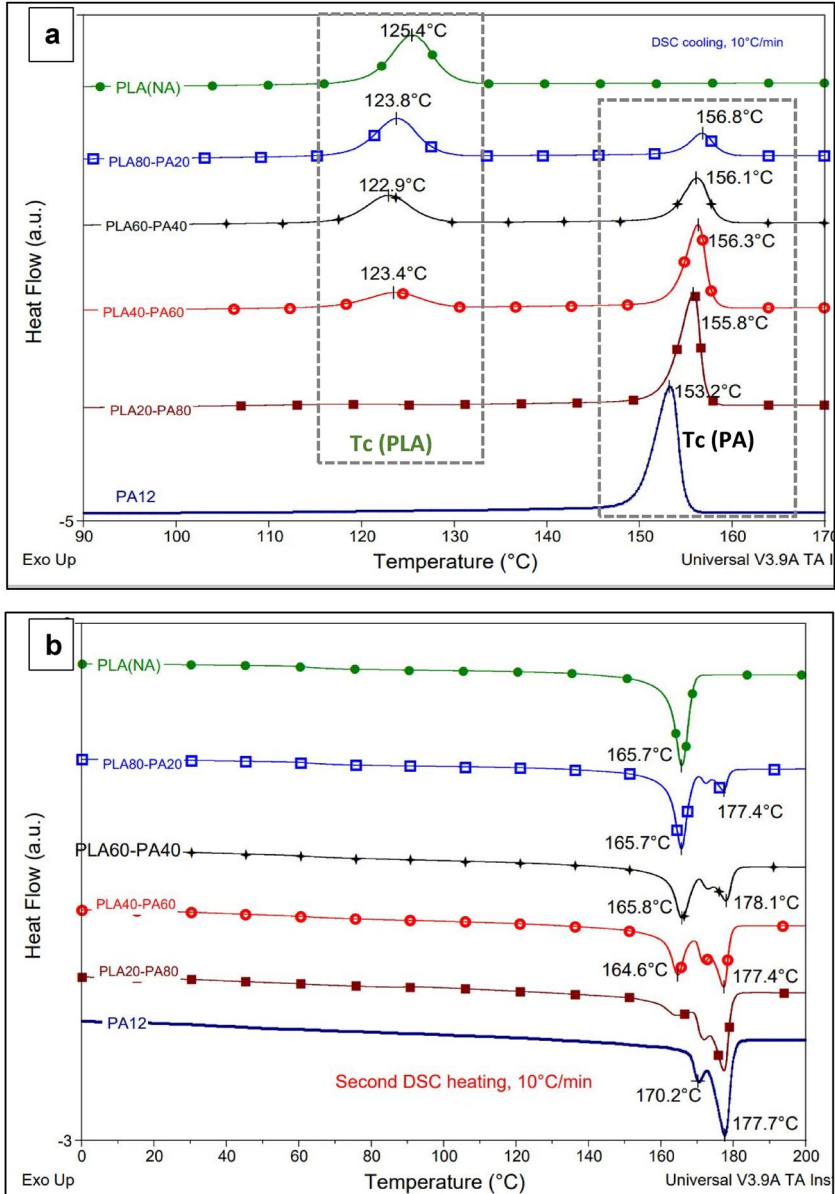


**Figure 10.** DSC traces recorded (a) during cooling and (b) second heating (10°C/min) of PLA(NA), PA12 and their blends.



### 3.2.3. DSC analyses to evidence the crystallization properties of PLA(NA)/PA blends

To evidence the added value obtained using PLA(NA), the results of non-isothermal characterizations will be concerned hereinafter. Figure 10(a, b) shows the DSC traces obtained during cooling from the molten state (Figure 10(a)) and following the second heating (Figure 10(b)) of PLA(NA), PA12, and their blends. PLA(NA)/PA blends show a first peak of crystallization ascribed to PA ( $T_{c(\text{PA})}$ ) at about 156 °C, whereas a second one ( $T_{c(\text{PLA})}$ ) at a temperature above 123 °C is attributed to PLA crystallization. Accordingly, the crystallization of each polymer takes place independently from each other. Still, for the blends rich in PA (i.e., PLA20–PA80), the crystallization of PLA is less detectable under the conditions of analysis. Undoubtedly, the presence of PLA(NA) in blends allows achieving an impressive DC during cooling (32–35%, Table 6), while those of PA are kept in the range 25–27%, thus it is assumed that the kinetics of crystallization are not much affected by the different PLA/PA ratios. Furthermore, in the subsequent DSC heating scans (Figure 10(b)) one cannot detect any exothermal events (additional cold crystallization process) meaning that the PLA has achieved a high level of crystallinity during the cooling step. Because the components of the blends are immiscible, the presence of two  $T_g$  is generally expected.  $T_g$  of PLA(NA) is kept around 62 °C (to note that it is more visible on the primary DSC curves), whereas the  $T_g$  of PA12, which is reported to be around 50 °C (Ma et al., 2020), was not detectable on the DSC traces. Although the main melting peaks of PLA and PA have not important changes, they are recorded respectively, at about 166 °C and 178 °C (a smaller shoulder is noted at 170 °C for PA). The double melting peaks of PA12 are linked to the existence of either a mixed crystal structure or a process related to the melting–recrystallization during heating (Ma et al., 2020). It is

**Table 6.** Quantification of DSC data following the characterization of PLA(NA), PA12 and their blends.

Sample	DSC cooling, 10 °C/min						Second DSC heating, 10 °C/min		
	$T_c$ °C (PLA)	$\Delta H_c$ J/g (PLA) <sup>a</sup>	$\chi_c$ % (PLA)	$T_c$ (PA)	$\Delta H_c$ J/g (PA) <sup>a</sup>	$\chi_c$ % (PA)	$T_g^{(\text{PLA})}$ °C	$T_{m'}$ °C (PLA)	$T_m$ °C (PA)
PLA(NA)	125	33.9	36.5	–	–	–	62	166	–
PLA80-PA20	124	32.0	34.4	157	52.0	24.9	63	166	172; 177
PLA60-PA40	123	32.2	34.6	156	53.2	25.5	63	166	173; 178
PLA40-PA60	124	29.5	31.7	156	53.8	25.7	62	165	172; 177
PLA20-PA80	117	NA	NA	156	55.4	26.5	62	164	171; 177
PA12	–	–	–	153	51.3	24.5	NA	–	170; 178

<sup>a</sup>Values normalized to the amounts of PLA or PA from samples.

also important to point out that the PLA/PA blends are totally in the molten state at above 180 °C, thus their processing by IM or extrusion can be easily achieved. For instance, the non-isothermal crystallization performed via DSC confirms the quick crystallization of PLA(NA)/PA and high DC of PLA (>30%). By comparison, in PLA (without NA)/PA blends, the polyester phase does not show any trace of crystallization (see [Supplementary material, Figure S2\(a, b\)](#)). Also, it is noteworthy mentioning that the comparative DSC isothermal tests at 120 °C of PLA(NA)/PA12 blends are once more proving the rapid crystallization of PA and PLA during quick cooling from the molten state, even before to attain the isothermal temperature of testing (see [Supplementary material, Figure S3](#)).

### **3.3. PLA(NA)/PA12 blends produced in the presence of selected compatibilizers and current prospects**

It is generally assumed that the polymer blends which show co-continuity of phases are of higher interest for applications, whereas on the other hand, important enhancements can be obtained in the presence of selected interfacial compatibilizers. Two additives claimed to tailor up the morphology and properties of PLA blends by reactive extrusion (REX) (Murariu, Paint, et al., 2015; Yemisci & Aytac, 2017), i.e., an epoxy styrene-acrylate oligomeric chain extender/compatibilizer, and a styrene - maleic anhydride random copolymer, have been tested at loadings of 2 wt.% to produce PLA(NA)/PA blends. The PLA(NA)/PA 60/40 wt.% compositions, which have shown a co-continuous structure (PLA60-PA40), were modified with 2%J and 2%XB under similar melt-mixing conditions. Regarding the thermal properties as evidenced by TGA, it was concluded that the addition and the presence of compatibilizers did not change the thermal stability of PLA(NA)/PA blends (results shown in [Supplementary material, Figure S4](#)). On the other hand, following the DSC analyses ([Figure 11\(a, b\)](#)), it was of first interest to demonstrate that the faster kinetics of crystallization of PLA are maintained. Indeed, the DSC traces recorded during cooling once more highlight the presence of two exothermal events assessing that both components, i.e., PA and PLA, preserve their crystallization ability ([Figure 11\(a\)](#)). However, it was reported elsewhere (Murariu, Paint, et al., 2015) that Joncryl can have some contribution in delaying the crystallization of PLA. This is confirmed by comparing PLA60-PA40/2%J and PLA60-PA40 samples: in the presence of 2%J the  $T_c$  of PLA component is about 119 °C (DC of 28%), whereas without J a slightly higher  $T_c$  and DC (123 °C and 34.6%, respectively) is noticed. The differences (linked to the presence or absence of J) can

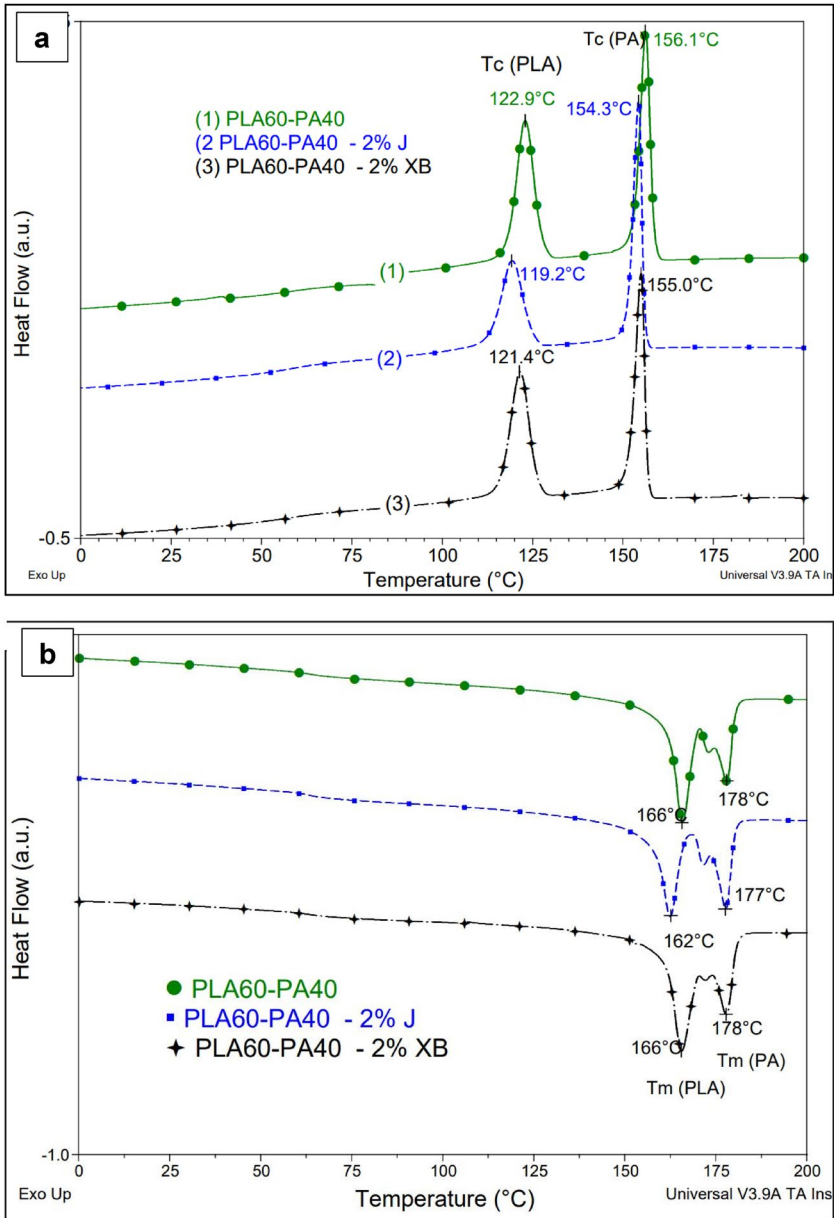


**Figure 11.** DSC traces recorded during cooling (a) and second heating (b) of PLA60-PA40 blends with/without compatibilizers.

be ascribed to the effects of this specific epoxy multifunctional additive claimed to increase the molecular weights of polyester (PLA) and PAs, which can explain the slight reduction in PLA crystallization. Moreover, following the chemical reactions between the epoxy functions and the

end groups of both polymers, J acts as compatibilizer. Regarding the crystallization of PA component, a slight change of the DC from about 25% (sample without compatibilizer) to 22% was evidenced in the presence of the compatibilizer. Still, from the comparative DSC traces recorded during heating scans (Figure 11(b)), it is seen that the PLA component was already crystallized during the (previous) cooling process. The endothermal transformations linked to the fusion of PLA and PA are overlapped, with distinct peaks corresponding to the melting of PLA (162–166 °C) and of PA (177–178 °C).

Concerning the information provided by SEM analyses (Figure 12(a–f)), it comes out that addition of either J or XB leads to important modifications of morphology. These differences are clearly observed for samples

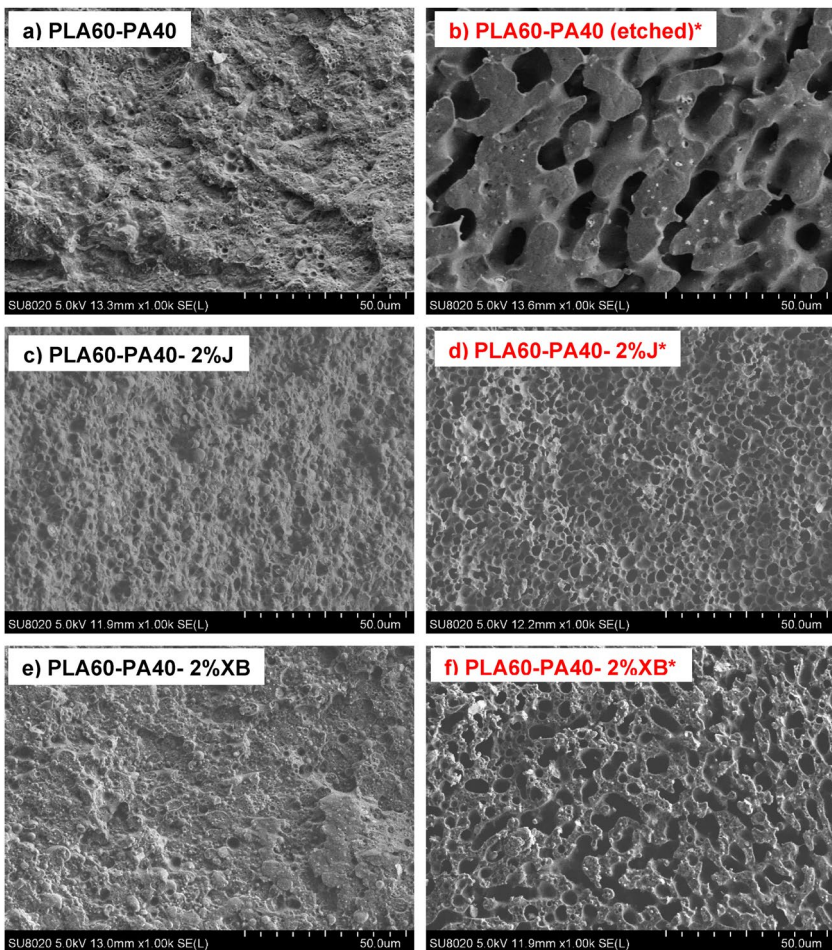


**Figure 12.** SEM images of PLA(NA)/PA12 60/40 wt.% with and without compatibilizers: (a, c, e) “non-etched” samples and (b, d, f) “etched” samples\* in chloroform.

previously “etched” in chloroform (Figure 12(b) compared to Figure 12(d) and (f)). Accordingly, it is seen that the initial co-continuous structure of PLA60–PA40 sample (Figure 12(b)) is dramatically modified especially by adding Joncryl (Figure 12(d)). Indeed, the large co-continuous and interpenetrated structures of PLA and PA are replaced by a “nodular” morphology, with PLA domains of  $2.5 (\pm 0.7) \mu\text{m}$  uniformly distributed through the PA phase. Based on our results and those reported in the frame of other studies (Murariu, Paint, et al., 2015; Rasselet et al., 2019), it can be claimed that the epoxy functional styrene-acrylic oligomers are efficient reactive compatibilizers and chain extenders for PLA blends, because they effectively improve the compatibility and interactions between components, while they lead to significant modifications of morphology and properties. In fact, during melt compounding by REX the glycidyl functions react with the end groups of PLA and/or of PA, therefore, the valuable role of Joncryl is complex: a) compatibilizer, giving better tensile strength, ductility and impact resistance (see hereinafter, Table 7); b) chain extender, leading to the preservation/increasing of molecular weights. On the other hand, in relation to the samples containing 2%XB, the SEM images (“etched” samples, Figure 12(f)) confirm the modification of morphology by the presence of lower and thinner regions of co-continuity and by apparition of PLA domains of different geometries and size, inside of PA regions.

Before concluding, it is important to remind that the PLA(NA)/PA12 blends (with/without compatibilizers) concerned by this study have been produced using micro-compounders. Therefore, the amounts of extruded material are limited to ca. 6 g and used only for specific characterizations requiring low quantities of products. This is the reason why it has been decided in the frame of current prospects to produce two other PLA(NA)/PA blends, in the presence or absence of Joncryl as compatibilizer, using a Brabender kneader for melt-compounding. Interestingly, the characterization of mechanical properties (Table 7) of PLA(NA)/PA-2%J blends confirms their high tensile strength (52 MPa) and rigidity (Young’s modulus  $\approx 1900$  MPa), values that are of interest for engineering applications,

**Table 7.** Comparative mechanical properties<sup>a</sup> of PLA(NA), PA12, and PLA(NA)/PA (50/50%.vol) blends with/without 2% Joncryl.

Sample	Max. tensile strength, MPa	Nominal strain at break, %	Young’s modulus, MPa	Izod impact resistance, kJ/m <sup>2</sup>
PLA(NA)	$61 \pm 1$	$3.6 \pm 0.8$	$2380 \pm 60$	$2.6 \pm 0.3$
PLA(NA)/PA 50/50	$45 \pm 1$	$6.5 \pm 1.2$	$2000 \pm 60$	$2.5 \pm 0.1$
PLA(NA)/PA-2%J	$52 \pm 2$	$175 \pm 22$	$1930 \pm 40$	$4.4 \pm 0.2$
PA12	$46 \pm 2$	$183 \pm 14$	$1390 \pm 80$	$3.7 \pm 0.2$

<sup>a</sup>Specimens cutted from plates made by compression moulding. Tensile properties: ASTM D638,  $v = 1$  mm/min, specimens type V; Izod – (notched) impact resistance: ASTM D256 (Method A, 3.46 m/s impact speed, 0.668 kg hammer).

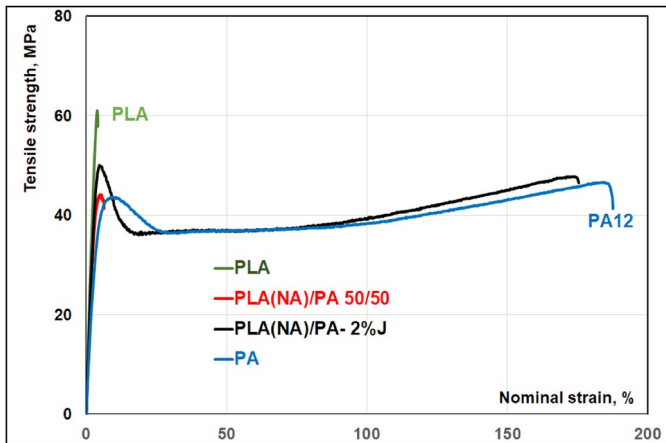


**Figure 13.** Tensile strength–strain curves obtained following the mechanical characterization of PLA(NA), PA12, and PLA(NA)/PA (50/50 % vol.) blends with/without 2% Joncryl.

and which are better than those of neat PA12 (46 MPa and 1400 MPa, respectively). Furthermore, by comparing PLA(NA)/PA-2%J to PLA(NA) or to the uncompatibilized blend, a substantial increase in ductility was recorded in the presence of the compatibilizer (Figure 13), from ca. 4% strain at the break (for PLA(NA)), to above 170% for the compatibilized blend. Besides, the enhancement of the impact resistance was noticed, even on specimens obtained by compression moulding.

However, it will be important to produce larger quantities of the most adapted PLA(NA)/PA blends and to evidence their performances using optimized processing conditions and particular methods of characterization (Dynamic Mechanical Analysis (DMA), HDT, Vicat softening temperature, etc.). The investigation of crystallization mechanisms using other techniques of analysis (polarized optical microscopy (POM), X-ray diffraction (XRD), etc.) is also of real interest.

Regarding the next prospects, the examination of biodegradation of PLA/PA blends is a subject of further attention, because up to now the relevant studies are missing. For instance, the key objective of different research groups was to improve the properties and morphology of PLA-based blends. Because the PLA/PA blends are proposed especially for durable/engineering applications, the wastes from these products can be also revalorized by mechanical or chemical recycling. Going from the results of this first study, it is considered that forthcoming contributions (already in progress) will lead to additional information regarding the added value of PLA(NA)/PA blends for durable applications.

## 4. Conclusions

To enlarge the use of PLA in durable applications, this study has highlighted the possibility to produce novel partly bio-based PLA/PA12 blends. One key originality is linked to the involvement of formulated PLA characterized by high crystallization ability. In this goal, a commercial PLA was modified with different NAs such as talc, sodium benzoate, PPA-Zn, and other products for identification of the most promising candidate in inducing PLA crystallization. PPA-Zn is of high effectiveness as NA, because it allows rapid PLA crystallization at high temperature ( $T_c = 124^\circ\text{C}$ ), while an impressive DC (>40%) is achieved. Larger quantities of PLA(NA) were produced via a laboratory/pilot twin-screw extruder as raw material and characterized by DSC, before and after IM tests. By annealing in the mould for 1–2 min at  $100\text{--}120^\circ\text{C}$  (an important requirement), PLA(NA) shows unconventional kinetics of crystallization and high DC (38–47%), whereas its half-crystallization time determined by DSC is lower than 1 min (at  $120\text{--}130^\circ\text{C}$ ).

PLA(NA) was used to produce PLA/PA12 blends using a laboratory micro-compounder. PLA and PA are immiscible, but compatible, thus a special attention was devoted to the understanding of specific morphologies obtained at different PLA(NA)/PA ratios. At low content (i.e., 20 wt.%) of PLA or PA, the blends show a typical “sea-island” morphology with droplets (of larger or smaller size) well distributed within the major component. The co-continuous structures are well evidenced at PLA/PA 60/40 ratio, whereas the evidence of PI was confirmed for PLA/PA 50/50 blends. Addition of specific compatibilizers such as epoxy styrene-acrylate oligomers (Joncryl) dramatically changed the morphology of blends, while beneficial mechanical properties are reported in current prospects (high tensile strength, ductility, impact resistance). The thermal characterizations confirm the adequate stability of PLA/PA blends at high temperature (TGA) and distinct zones of degradation corresponding to both components. Using non-isothermal DSC characterizations, a successive crystallization process of PA ( $T_c \approx 156^\circ\text{C}$ ) and of PLA ( $T_c \approx 124^\circ\text{C}$ ) is observed. All DSC measurements of PLA(NA)/PA blends suggest powerful nucleation ability and crystallization kinetics ascribed to the addition of PLA(NA). Following the combination of PLA(NA) with an engineering polymer of interest (PA12), it is expected to produce new (partially) bio-based materials showing improved processing due to enhanced PLA crystallization and fine microcrystalline structure, and better thermal, mechanical, and barrier properties. For instance, based on the current prospects, it is believed that the PLA(NA)/PA ratios, addition of adequate compatibilizers, mixing, and processing conditions, are among the key factors determining the morphology of blends, thermal, and mechanical

properties. The PLA(NA)/PA engineered blends are under development, therefore additional investigations are for further consideration.

## Acknowledgements

The authors thank Anne-Laure Dechief, Julie Passion, and Loïc Brison for assistance in realization of experiments, and all mentioned companies for supplying raw materials.

## Disclosure statement

No potential conflict of interest was reported by the authors.

## Funding

The authors thank the Wallonia Region, Nord-Pas de Calais Region and European Community for the financial support in the frame of INTERREG IV – Grant NANOLAC FW 1.1.8 and their collaborators. This work has been partly supported by the European Commission and Wallonia Region: FEDER program 2014–2020 under the Grants PROSTEM (Multifunctional films (FMF), PROSTEM-4, Euroges: 3192) and MACOBIO (Low Carbon Footprint Materials).

## References

- Ageyeva, T., Kovács, J. G., & Tábi, T. (2022). Comparison of the efficiency of the most effective heterogeneous nucleating agents for poly(lactic acid). *Journal of Thermal Analysis and Calorimetry*, 147(15), 8199–8211. <https://doi.org/10.1007/s10973-021-11145-y>
- Auras, R., Harte, B., & Selke, S. (2004). An overview of polylactides as packaging materials. *Macromolecular Bioscience*, 4(9), 835–864. <https://doi.org/10.1002/mabi.200400043>
- Babu, R. P., O'Connor, K., & Seeram, R. (2013). Current progress on bio-based polymers and their future trends. *Progress in Biomaterials*, 2(1), 8. <https://doi.org/10.1186/2194-0517-2-8>.
- Battegazzore, D., Bocchini, S., & Frache, A. (2011). Crystallization kinetics of poly(lactic acid)-talc composites. *Express Polymer Letters*, 5(10), 849–858. <https://doi.org/10.3144/expresspolymlett.2011.84>
- Carrasco, F., Pagès, P., Gámez-Pérez, J., Santana, O. O., & MasPOCH, M. L. (2010). Processing of poly(lactic acid): Characterization of chemical structure, thermal stability and mechanical properties. *Polymer Degradation and Stability*, 95(2), 116–125. <https://doi.org/10.1016/j.polyimdegradstab.2009.11.045>
- Chanda, M., & Roy, S. (2008). 1 – Industrial Polymers. In M. Chanda & S. Roy (Eds), *Industrial polymers, specialty polymers, and their applications* (1st ed., pp. 1–159). CRC Press. <https://doi.org/10.1201/9781420080599>
- Chen, P., Zhou, H., Liu, W., Zhang, M., Du, Z., & Wang, X. (2015). The synergistic effect of zinc oxide and phenylphosphonic acid zinc salt on the crystallization behavior of poly (lactic acid). *Polymer Degradation and Stability*, 122, 25–35. <https://doi.org/10.1016/j.polyimdegradstab.2015.10.014>



- Degli Esposti, M., Morselli, D., Fava, F., Bertin, L., Cavani, F., Viaggi, D., & Fabbri, P. (2021). The role of biotechnology in the transition from plastics to bioplastics: An opportunity to reconnect global growth with sustainability. *FEBS Open Bio*, 11(4), 967–983. <https://doi.org/10.1002/2211-5463.13119>.
- Drumright, R. E., Gruber, P. R., & Henton, D. E. (2000). Polylactic acid technology. *Advanced Materials*, 12(23), 1841–1846. [https://doi.org/10.1002/1521-4095\(200012\)12:23<1841::AID-ADMA1841>3.0.CO;2-E](https://doi.org/10.1002/1521-4095(200012)12:23<1841::AID-ADMA1841>3.0.CO;2-E)
- Feng, F., & Ye, L. (2010). Structure and property of polylactide/polyamide blends. *Journal of Macromolecular Science, Part B*, 49(6), 1117–1127. <https://doi.org/10.1080/00222341003609179>
- Fenni, S. E., Cavallo, D., & Müller, A. J. (2019). Nucleation and crystallization in bio-based immiscible polyester blends. In M. L. Di Lorenzo & R. Androsch (Eds.), *Thermal properties of bio-based polymers* (pp. 219–256). Springer International Publishing.
- Gonzalez-Garzon, M., Shahbikian, S., & Huneault, M. A. (2018). Properties and phase structure of melt-processed PLA/PMMA blends. *Journal of Polymer Research*, 25(2), 1–13. <https://doi.org/10.1007/s10965-018-1438-1>
- Gug, J., & Sobkowicz, M. J. (2016). Improvement of the mechanical behavior of bioplastic poly(lactic acid)/polyamide blends by reactive compatibilization. *Journal of Applied Polymer Science*, 133(45). <https://doi.org/10.1002/app.43350>
- Gupta, B., Revagade, N., & Hilborn, J. (2007). Poly(lactic acid) fiber: An overview. *Progress in Polymer Science*, 32(4), 455–482. <https://doi.org/10.1016/j.progpolymsci.2007.01.005>
- Halley, P. J., & Dorgan, J. R. (2011). Next-generation biopolymers: Advanced functionality and improved sustainability. *MRS Bulletin*, 36(9), 687–691. <https://doi.org/10.1557/mrs.2011.180>
- Harris, A. M., & Lee, E. C. (2008). Improving mechanical performance of injection molded PLA by controlling crystallinity. *Journal of Applied Polymer Science*, 107(4), 2246–2255. <https://doi.org/10.1002/app.27261>
- Hashima, K., Nishitsuji, S., & Inoue, T. (2010). Structure-properties of super-tough PLA alloy with excellent heat resistance. *Polymer*, 51(17), 3934–3939. <https://doi.org/10.1016/j.polymer.2010.06.045>
- Hassan, A., Balakrishnan, H., & Akbari, A. (2013). Polylactic acid based blends, composites and nanocomposites. In S. Thomas, P. M. Visakh, & A. P. Mathew (Eds.), *Advances in natural polymers: Composites and nanocomposites* (pp. 361–396). Springer Berlin Heidelberg.
- Jalali Dil, E., Carreau, P. J., & Favis, B. D. (2015). Morphology, miscibility and continuity development in poly(lactic acid)/poly(butylene adipate-co-terephthalate) blends. *Polymer*, 68, 202–212. <https://doi.org/10.1016/j.polymer.2015.05.012>
- Jamshidian, M., Tehrani, E. A., Imran, M., Jacquot, M., & Desobry, S. (2010). Poly-lactic acid: Production, applications, nanocomposites, and release studies. *Comprehensive Reviews in Food Science and Food Safety*, 9(5), 552–571. <https://doi.org/10.1111/j.1541-4337.2010.00126.x>
- Jiang, L., Shen, T., Xu, P., Zhao, X., Li, X., Dong, W., ... Chen, M. (2016). Crystallization modification of poly(lactide) by using nucleating agents and stereocomplexation. *e-Polymers*, 16(1), 1–13. <https://doi.org/10.1515/epoly-2015-0179>

- Jo, M. Y., Ryu, Y. J., Ko, J. H., & Yoon, J.-S. (2012). Effects of compatibilizers on the mechanical properties of abs/PLA composites. *Journal of Applied Polymer Science*, 125(S2), E231–E238. <https://doi.org/10.1002/app.36732>
- Koronis, G., Silva, A., & Fontul, M. (2013). Green composites: A review of adequate materials for automotive applications. *Composites Part B: Engineering*, 44(1), 120–127. <https://doi.org/10.1016/j.compositesb.2012.07.004>
- Kusumi, R., Teranishi, S., Kimura, F., Wada, M., Kimura, T., Horikawa, Y., & Kawai, T. (2018). Crystal orientation of poly(l-lactic acid) induced by magnetic alignment of a nucleating agent. *Polymers*, 10(6), 653. <https://doi.org/10.3390/polym10060653>
- Lasprilla, A. J. R., Martinez, G. A. R., Lunelli, B. H., Jardini, A. L., & Filho, R. M. (2012). Poly-lactic acid synthesis for application in biomedical devices – A review. *Biotechnology Advances*, 30(1), 321–328. <https://doi.org/10.1016/j.biotechadv.2011.06.019>
- Li, H., & Huneault, M. A. (2007). Effect of nucleation and plasticization on the crystallization of poly(lactic acid). *Polymer*, 48(23), 6855–6866. <https://doi.org/10.1016/j.polymer.2007.09.020>
- Lim, L. T., Auras, R., & Rubino, M. (2008). Processing technologies for poly(lactic acid). *Progress in Polymer Science*, 33(8), 820–852. <https://doi.org/10.1016/j.progpolymsci.2008.05.004>
- Luo, F., Fortenberry, A., Ren, J., & Qiang, Z. (2020). Recent progress in enhancing poly(lactic acid) stereocomplex formation for material property improvement. *Frontiers in Chemistry*, 8, 688. <https://doi.org/10.3389/fchem.2020.00688>
- Ma, N., Liu, W., Ma, L., He, S., Liu, H., Zhang, Z., ... Zhu, C. (2020). Crystal transition and thermal behavior of nylon 12. *e-Polymers*, 20(1), 346–352. <https://doi.org/10.1515/epoly-2020-0039>
- McLauchlin, A. R., & Ghita, O. R. (2016). Studies on the thermal and mechanical behavior of PLA-PET blends. *Journal of Applied Polymer Science*, 133(43), Article ID 44147, 1–11. <https://doi.org/10.1002/app.44147>
- Morão, A., & de Bie, F. (2019). Life cycle impact assessment of polylactic acid (PLA) produced from sugarcane in Thailand. *Journal of Polymers and the Environment*, 27(11), 2523–2539. <https://doi.org/10.1007/s10924-019-01525-9>
- Murariu, M., Bonnaud, L., Yoann, P., Fontaine, G., Bourbigot, S., & Dubois, P. (2010). New trends in polylactide (PLA)-based materials: “Green” PLA–calcium sulfate (nano)composites tailored with flame retardant properties. *Polymer Degradation and Stability*, 95(3), 374–381. <https://doi.org/10.1016/j.polyimdegradstab.2009.11.032>
- Murariu, M., & Dubois, P. (2016). PLA composites: From production to properties. *Advanced Drug Delivery Reviews*, 107, 17–46. <https://doi.org/10.1016/j.addr.2016.04.003>
- Murariu, M., Dechief, A.-L., Ramy-Ratierison, R., Paint, Y., Raquez, J.-M., & Dubois, P. (2015). Recent advances in production of poly(lactic acid) (PLA) nanocomposites: A versatile method to tune crystallization properties of PLA. *Nanocomposites*, 1(2), 71–82. <https://doi.org/10.1179/2055033214Y.0000000008>
- Murariu, M., Doumbia, A., Bonnaud, L., Dechief, A. L., Paint, Y., Ferreira, M., ... Dubois, P. (2011). High-performance polylactide/ZnO nanocomposites designed for films and fibers with special end-use properties. *Biomacromolecules*, 12(5), 1762–1771. <https://doi.org/10.1021/bm2001445>
- Murariu, M., Laoutid, F., Dubois, P., Fontaine, G., Bourbigot, S., Devaux, E., ... Solarski, S. (2014). Chapter 21 – Pathways to biodegradable flame retardant

- polymer (nano)composites. In C. D. Papaspyrides & P. Kiliaris (Eds.), *Polymer green flame retardants* (pp. 709–773). Elsevier.
- Murariu, M., Paint, Y., Murariu, O., Raquez, J.-M., Bonnaud, L., & Dubois, P. (2015). Current progress in the production of PLA–ZnO nanocomposites: Beneficial effects of chain extender addition on key properties. *Journal of Applied Polymer Science*, 132(48), Article ID 42480, 1–11. <https://doi.org/10.1002/app.42480>
- Nagarajan, V., Mohanty, A. K., & Misra, M. (2016). Perspective on polylactic acid (PLA) based sustainable materials for durable applications: Focus on toughness and heat resistance. *ACS Sustainable Chemistry & Engineering*, 4(6), 2899–2916. <https://doi.org/10.1021/acssuschemeng.6b00321>
- Nam, B.-U., & Son, Y. (2020). Enhanced impact strength of compatibilized poly(lactic acid)/polyamide 11 blends by a crosslinking agent. *Journal of Applied Polymer Science*, 137(35), 49011. <https://doi.org/10.1002/app.49011>
- Pantani, R., Gorrasi, G., Vigliotta, G., Murariu, M., & Dubois, P. (2013). PLA–ZnO nanocomposite films: Water vapor barrier properties and specific end-use characteristics. *European Polymer Journal*, 49(11), 3471–3482. <https://doi.org/10.1016/j.eurpolymj.2013.08.005>
- Patel, R., Ruehle, D. A., Dorgan, J. R., Halley, P., & Martin, D. (2014). Biorenewable blends of polyamide-11 and polylactide. *Polymer Engineering & Science*, 54(7), 1523–1532. <https://doi.org/10.1002/pen.23692>
- Penco, M., Spagnoli, G., Peroni, I., Rahman, M. A., Frediani, M., Oberhauser, W., & Lazzeri, A. (2011). Effect of nucleating agents on the molar mass distribution and its correlation with the isothermal crystallization behavior of poly(l-lactic acid). *Journal of Applied Polymer Science*, 122(6), 3528–3536. <https://doi.org/10.1002/app.34761>
- Qu, Z., Bu, J., Pan, X., & Hu, X. (2018). Probing the nanomechanical properties of PLA/PC blends compatibilized with compatibilizer and nucleation agent by AFM. *Journal of Polymer Research*, 25(6), 138. <https://doi.org/10.1007/s10965-018-1529-z>
- Raj, A., Samuel, C., Malladi, N., & Prashantha, K. (2020). Enhanced (thermo) mechanical properties in biobased poly(l-lactide)/poly(amide-12) blends using high shear extrusion processing without compatibilizers. *Polymer Engineering & Science*, 60(8), 1902–1916. <https://doi.org/10.1002/pen.25426>
- Raj, A., Samuel, C., & Prashantha, K. (2020). Role of compatibilizer in improving the properties of PLA/PA12 blends. *Frontiers in Materials*, 7, Article ID 193, 1–12. <https://doi.org/10.3389/fmats.2020.00193>
- Raquez, J.-M., Habibi, Y., Murariu, M., & Dubois, P. (2013). Polylactide (PLA)-based nanocomposites. *Progress in Polymer Science*, 38(10–11), 1504–1542. <https://doi.org/10.1016/j.progpolymsci.2013.05.014>
- Rasal, R. M., Janorkar, A. V., & Hirt, D. E. (2010). Poly(lactic acid) modifications. *Progress in Polymer Science*, 35(3), 338–356. <https://doi.org/10.1016/j.progpolymsci.2009.12.003>
- Rasselet, D., Caro-Bretelle, A.-S., Taguet, A., & Lopez-Cuesta, J.-M. (2019). Reactive compatibilization of PLA/PA11 blends and their application in additive manufacturing. *Materials*, 12(3), 485. <https://doi.org/10.3390/ma12030485>
- Rezvani Ghomi, E., Khosravi, F., Saedi Ardahaei, A., Dai, Y., Neisiany, R. E., Foroughi, F., ... Ramakrishna, S. (2021). The life cycle assessment for poly-

- lactic acid (PLA) to make it a low-carbon material. *Polymers*, 13(11), 1854. <https://doi.org/10.3390/polym13111854>
- Rydz, J., Sikorska, W., Kyulavska, M., & Christova, D. (2014). Polyester-based (bio)degradable polymers as environmentally friendly materials for sustainable development. *International Journal of Molecular Sciences*, 16(1), 564–596. <https://doi.org/10.3390/ijms16010564>
- Saeidlou, S., Huneault, M. A., Li, H., & Park, C. B. (2012). Poly(lactic acid) crystallization. *Progress in Polymer Science*, 37(12), 1657–1677. <https://doi.org/10.1016/j.progpolymsci.2012.07.005>
- Saini, P., Arora, M., & Kumar, M. N. V. R. (2016). Poly(lactic acid) blends in biomedical applications. *Advanced Drug Delivery Reviews*, 107, 47–59. <https://doi.org/10.1016/j.addr.2016.06.014>
- Samuel, C., Raquez, J.-M., & Dubois, P. (2013). PLLA/PMMA blends: A shear-induced miscibility with tunable morphologies and properties? *Polymer*, 54(15), 3931–3939. <https://doi.org/10.1016/j.polymer.2013.05.021>
- Sangroniz, L., Gancheva, T., Favis, B. D., Müller, A. J., & Santamaria, A. (2021). Rheology of complex biobased quaternary blends: Poly(lactic acid) [poly(ethylene oxide)]/poly(ether-b-amide)/poly(amide 11). *Journal of Rheology*, 65(3), 437–451. <https://doi.org/10.1122/8.0000202>
- Shaghaleh, H., Xu, X., & Wang, S. (2018). Current progress in production of biopolymeric materials based on cellulose, cellulose nanofibers, and cellulose derivatives. *RSC Advances*, 8(2), 825–842. <https://doi.org/10.1039/C7RA11157F>
- Shakoor, A., & Thomas, N. L. (2014). Talc as a nucleating agent and reinforcing filler in poly(lactic acid) composites. *Polymer Engineering & Science*, 54(1), 64–70. <https://doi.org/10.1002/pen.23543>
- Silva, T. F. d., Menezes, F., Montagna, L. S., Lemes, A. P., & Passador, F. R. (2019). Preparation and characterization of antistatic packaging for electronic components based on poly(lactic acid)/carbon black composites. *Journal of Applied Polymer Science*, 136(13), 47273. <https://doi.org/10.1002/app.47273>
- Stoclet, G., Seguela, R., & Lefebvre, J. M. (2011). Morphology, thermal behavior and mechanical properties of binary blends of compatible biosourced polymers: Polylactide/polyamide11. *Polymer*, 52(6), 1417–1425. <https://doi.org/10.1016/j.polymer.2011.02.002>
- Suryanegara, L., Okumura, H., Nakagaito, A. N., & Yano, H. (2011). The synergetic effect of phenylphosphonic acid zinc and microfibrillated cellulose on the injection molding cycle time of PLA composites. *Cellulose*, 18(3), 689–698. <https://doi.org/10.1007/s10570-011-9515-1>
- Teixeira, S., Eblagon, K. M., Miranda, F. R., Pereira, M. F., & Figueiredo, J. L. (2021). Towards controlled degradation of poly(lactic) acid in technical applications. *Journal of Carbon Research*, 7(2), 42. <https://doi.org/10.3390/c7020042>
- Tejada-Oliveros, R., Gomez-Caturla, J., Sanchez-Nacher, L., Montanes, N., & Quiles-Carrillo, L. (2021). Improved toughness of polylactide by binary blends with polycarbonate with glycidyl and maleic anhydride-based compatibilizers. *Macromolecular Materials and Engineering*, 306(12), 2100480. <https://doi.org/10.1002/mame.202100480>
- Tomita, K., Hayashi, N., Ikeda, N., & Kikuchi, Y. (2003). Isolation of a thermophilic bacterium degrading some nylons. *Polymer Degradation and Stability*, 81(3), 511–514. [https://doi.org/10.1016/S0141-3910\(03\)00151-4](https://doi.org/10.1016/S0141-3910(03)00151-4)

- Tripathi, N., Misra, M., & Mohanty, A. K. (2021). Durable polylactic acid (PLA)-based sustainable engineered blends and biocomposites: Recent developments, challenges, and opportunities. *ACS Engineering Au*, 1(1), 7–38. <https://doi.org/10.1021/acsengineeringau.1c00011>
- Ucpinar Durmaz, B., & Aytac, A. (2022). Investigation of the mechanical, thermal, morphological and rheological properties of bio-based polyamide11/poly(lactic acid) blend reinforced with short carbon fiber. *Materials Today Communications*, 30, 103030. <https://doi.org/10.1016/j.mtcomm.2021.103030>
- Walha, F., Lamnawar, K., Maazouz, A., & Jaziri, M. (2016). Rheological, morphological and mechanical studies of sustainably sourced polymer blends based on poly(lactic acid) and polyamide 11. *Polymers*, 8(3), 61. <https://doi.org/10.3390/polym8030061>
- Wei, X.-F. D., Vico, L., Larroche, P., Kallio, K. J., Bruder, S., Bellander, M., ... Edenqvist, M. S. (2019). Ageing properties and polymer/fuel interactions of polyamide 12 exposed to (bio)diesel at high temperature. *Npj Materials Degradation*, 3(1) <https://doi.org/10.1038/s41529-018-0065-y>
- Wu, N., & Wang, H. (2013). Effect of zinc phenylphosphonate on the crystallization behavior of poly(l-lactide). *Journal of Applied Polymer Science*, 130(4), 2744–2752. <https://doi.org/10.1002/app.39471>
- Wypych, A., & Wypych, G. (2021). 3 – Nucleating agents. In A. Wypych & G. Wypych (Eds.), *Databook of nucleating agents* (2nd ed., pp. 17–376). ChemTec Publishing.
- Yemisci, F., & Aytac, A. (2017). Compatibilization of poly(lactic acid)/polycarbonate blends by different coupling agents. *Fibers and Polymers*, 18(8), 1445–1451. <https://doi.org/10.1007/s12221-017-6671-4>
- Yoo, H. M., Jeong, S.-Y., & Choi, S.-W. (2021). Analysis of the rheological property and crystallization behavior of polylactic acid (Ingeo™ biopolymer 4032D) at different process temperatures. *e-Polymers*, 21(1), 702–709. <https://doi.org/10.1515/epoly-2021-0071>
- Zhang, J., Yan, D.-X., Xu, J.-Z., Huang, H.-D., Lei, J., & Li, Z.-M. (2012). Highly crystallized poly (lactic acid) under high pressure. *AIP Advances*, 2(4), 042159. <https://doi.org/10.1063/1.4769351>
- Zhao, X., Hu, H., Wang, X., Yu, X., Zhou, W., & Peng, S. (2020). Super tough poly(lactic acid) blends: A comprehensive review. *RSC Advances*, 10(22), 13316–13368. <https://doi.org/10.1039/D0RA01801E>.